

Ruthenium Carbene, Vinylidene, and Allenylidene Complexes with a Bis(3,5-dimethylpyrazol-1-yl)acetato Heteroscorpionate Ligand

Henning Kopf,[†] Cezary Pietraszuk,[‡] Eike Hübner,[§] and Nicolai Burzlaff*[§]

Department of Chemistry, University of Konstanz, Fach M728, D-78457 Konstanz, Germany, Faculty of Chemistry, Adam Mickiewicz University, Grunwaldzka 6, 60-780 Poznań, Poland, and Institute of Inorganic Chemistry, University of Erlangen-Nürnberg, Egerlandstrasse 1, D-91058 Erlangen, Germany

Received January 18, 2006

A series of neutral ruthenium(II) carbonyl, carbene, vinylidene, and allenylidene complexes [Ru(bdmpza)(Cl)(L)(PPh₃)] (L = C(OR')R, C=CHR, C=C=CR₂, CO) containing the bis(3,5-dimethylpyrazol-1-yl)acetato (bdmpza) ligand, an N,N,O heteroscorpionate ligand, have been prepared. Treatment of [Ru(bdmpza)(Cl)(PPh₃)₂] (**1a**) with a variety of alkynes HC≡CR (R = Ph, Tol, Pr, Bu) afforded the vinylidene complexes [Ru(bdmpza)(Cl)(=C=CHR)(PPh₃)] (**2a–d**). The carbonyl complex [Ru(bdmpza)(Cl)(CO)(PPh₃)] (**3**) is formed via oxidative or acid-induced degradation pathways from the vinylidene complexes. Reaction of **1a** with the hydroxy-functionalized alkynes HC≡C(CH₂)_nOH (n = 2, 3) yielded the cyclic Fischer type carbene complexes [Ru(bdmpza)(Cl)(=C(CH₂)₃O)(PPh₃)] (**4a**) and [Ru(bdmpza)(Cl)(=C(CH₂)₄O)(PPh₃)] (**4b**). The ruthenium(II) allenylidene complexes [Ru(bdmpza)(Cl)(=C=C=CR₂)(PPh₃)] (**5a**, R = Ph; **5b**, R = Tol) were prepared by the reaction of **1a** with propargyl alcohols HC≡CC(R)₂OH via the vinylidene intermediates [Ru(bdmpza)(Cl)(=C=CHCR₂OH)(PPh₃)]. X-ray crystal structures of one structural isomer of the vinylidene complex [Ru(bdmpza)(Cl)(=C=CHTol)(PPh₃)] (**2b**), the carbonyl complex [Ru(bdmpza)(Cl)(CO)(PPh₃)] (**3**), the carbene complex [Ru(bdmpza)(Cl)(=C(CH₂)₄O)(PPh₃)] (**4b-I**), and two structural isomers of [Ru(bdmpza)(Cl)(=C=C=CPh₂)(PPh₃)] (**5a-I** and **5a-II**) are reported.

Introduction

The hydridotris(pyrazol-1-yl)borate (HB(pz)₃⁻; Tp) chemistry of ruthenium(II) has received considerable attention during the past decade.^{1–5} In particular, metallacumulenyldiene ruthenium

complexes⁶ bearing tridentate Tp or Tp-related ligands have been reported.^{7–12,42} The focus of these studies has been their catalytic activity in ring-closing metathesis (RCM) or ring-opening metathesis polymerization (ROMP).^{13–15} Thus, recently the neutral ruthenium benzylidene complex [RuCl{κ³-HB(pz)₃}(=CHPh)(PCy₃)] and related cationic complexes [Ru{κ³-HB(pz)₃}(=CHPh)(PCy₃)(L)]⁺ (L = H₂O, pyridine, CH₃CN) have been reported to be active in RCM.¹² The ruthenium benzylidene complex [RuCl{κ³-HB(pz)₃}(=CHPh)(ImesH₂)]

* To whom correspondence should be addressed. Tel.: (internat.) +49(0)9131/85-28976. Fax: (internat.) +49(0)9131/85-27387. E-mail: burzlaff@chemie.uni-erlangen.de.

[†] University of Konstanz.

[‡] Adam Mickiewicz University.

[§] University of Erlangen-Nürnberg.

(1) (a) Slugovc, C.; Schmid, R.; Kirchner, K. *Coord. Chem. Rev.* **1999**, *185–186*, 109–126. (b) Cadierno, V.; Díez, J.; Pilar Gamasa, M.; Gimeno, J.; Lastra, E. *Coord. Chem. Rev.* **1999**, *193–195*, 147–205. (c) Gemel, C.; Wiede, P.; Mereiter, K.; Sapunov, V. N.; Schmid, R.; Kirchner, K. *J. Chem. Soc., Dalton Trans.* **1996**, 4071–4076. (d) Corrochano, A. E.; Jalón, F. A.; Otero, A.; Kubicki, M. M.; Richard, P. *Organometallics* **1997**, *16*, 145–148. (e) Chen, Y.-Z.; Chan, W. C.; Lau, C. P.; Chu, H. S.; Lee, H. L. *Organometallics* **1997**, *16*, 1241–1246. (f) Trimmel, G.; Slugovc, C.; Wiede, P.; Mereiter, K.; Sapunov, V. N.; Schmid, R.; Kirchner, K. *Inorg. Chem.* **1997**, *36*, 1076–1083. (g) Gemel, C.; Kickelbick, G.; Schmid, R.; Kirchner, K. *J. Chem. Soc., Dalton Trans.* **1997**, 2113–2117. (h) Slugovc, C.; Mauthner, K.; Kacel, M.; Mereiter, K.; Schmid, R.; Kirchner, K. *Chem. Eur. J.* **1998**, *4*, 2043–2050. (i) Slugovc, C.; Mereiter, K.; Schmid, R.; Kirchner, K. *J. Am. Chem. Soc.* **1998**, *120*, 6175–6176. (j) Lo, Y.-H.; Lin, Y.-C.; Lee, G.-H.; Wang, Y. *Organometallics* **1999**, *18*, 982–988. (k) Slugovc, C.; Gemel, C.; Shen, J.-Y.; Doberer, D.; Schmid, R.; Kirchner, K.; Mereiter, K. *Monatsh. Chem.* **1999**, *130*, 363–375. (l) Slugovc, C.; Mereiter, K.; Schmid, R.; Kirchner, K. *Eur. J. Inorg. Chem.* **1999**, 1141–1149.

(2) Slugovc, C.; Mereiter, K.; Zobetz, E.; Schmid, R.; Kirchner, K. *Organometallics* **1996**, *15*, 5275–5277.

(3) Slugovc, C.; Doberer, D.; Gemel, C.; Schmid, R.; Kirchner, K.; Winkler, B.; Stelzer, F. *Monatsh. Chem.* **1998**, *129*, 221–233.

(4) Buriez, B.; Burns, I. D.; Hill, A. F.; White, A. J. P.; Williams, D. J.; Wilton-Ely, J. D. E. *Organometallics* **1999**, *18*, 1504–1516.

(5) Pavlik, S.; Gemel, C.; Slugovc, C.; Mereiter, K.; Schmid, R.; Kirchner, K. *J. Organomet. Chem.* **2001**, *617–618*, 301–310.

(6) (a) Bruce, M. I. *Chem. Rev.* **1991**, *91*, 197–257. (b) Bruce, M. I. *Chem. Rev.* **1998**, *98*, 2797–2858. (c) Touchard, D.; Dixneuf, P. H. *Coord. Chem. Rev.* **1998**, *178–180*, 409–429. (d) Puerta, M. C.; Valerga, P. *Coord. Chem. Rev.* **1999**, *193–195*, 977–1025. (e) Cadierno, V.; Pilar Gamasa, M.; Gimeno, J. *Eur. J. Inorg. Chem.* **2001**, 571–591. (f) Rigaut, S.; Touchard, D.; Dixneuf, P. H. *Coord. Chem. Rev.* **2004**, *248*, 1585–1601. (g) Cadierno, V.; Pilar Gamasa, M.; Gimeno, J. *Coord. Chem. Rev.* **2004**, *248*, 1627–1657.

(7) (a) Guerchias, V. *Eur. J. Inorg. Chem.* **2002**, 783–796. (b) Slugovc, C.; Mereiter, K.; Schmid, R.; Kirchner, K. *Organometallics* **1998**, *17*, 827–831. (c) Rüba, E.; Gemel, C.; Slugovc, C.; Mereiter, K.; Schmid, R.; Kirchner, K. *Organometallics* **1999**, *18*, 2275–2280. (d) Sanford, M. S.; Valdez, M. R.; Grubbs, R. H. *Organometallics* **2001**, *20*, 5455–5463.

(8) Slugovc, C.; Sapunov, V. N.; Wiede, P.; Mereiter, K.; Schmid, R.; Kirchner, K. *J. Chem. Soc., Dalton Trans.* **1997**, 4209–4216.

(9) Buriez, B.; Cook, D. J.; Harlow, K. J.; Hill, A. F.; Welton, T.; White, A. J. P.; Williams, D. J.; Wilton-Ely, J. D. E. *J. Organomet. Chem.* **1999**, *578*, 264–267.

(10) Harlow, K. J.; Hill, A. F.; Wilton-Ely, J. D. E. *J. Chem. Soc., Dalton Trans.* **1999**, 285–291.

(11) Jiménez-Tenorio, M. A.; Jiménez-Tenorio, M.; Puerta, M. C.; Valerga, P. *Organometallics* **2000**, *19*, 1333–1342.

(12) Sanford, M. S.; Henling, L. M.; Grubbs, R. H. *Organometallics* **1998**, *17*, 5384–5389.

(13) Bruneau, C.; Dixneuf, P. H. *Acc. Chem. Res.* **1999**, *32*, 311–323.

(14) Fürstner, A. *Angew. Chem., Int. Ed.* **2000**, *39*, 3012–3043.

(15) Katayama, H.; Yoshida, T.; Ozawa, F. *J. Organomet. Chem.* **1998**, *562*, 203–206.

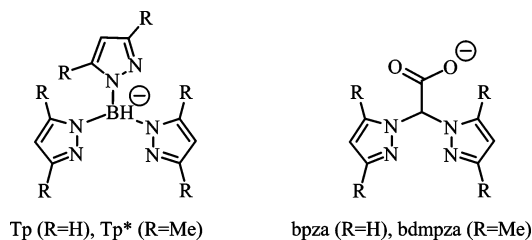


Figure 1. Analogy between hydridotris(pyrazol-1-yl)borato and bis(pyrazol-1-yl)acetato ligands.

with a coordinated N-heterocyclic carbene (NHC) has been described as well.¹⁶ Another ruthenium vinylidene complex, $[\text{RuCl}\{\kappa^3\text{-HB}(\text{pz})_3\}(\text{C}=\text{CHPh})(\text{PPh}_3)]$, was found to catalyze ROMP of norbornene.¹⁵ Due to the six-coordinated and thus coordinatively saturated metal center, the presence of cocatalysts such as HCl, CuCl, and AlCl_3 is required in all of these cases. Bis(pyrazol-1-yl)acetic acids, a new class of N,N,O heteroscorpionate ligand, have proved to be almost equivalent to the hydridotris(pyrazol-1-yl)borato ligands in their ligand properties.^{17–22} Since their introduction to coordination chemistry in 1999 by Otero,¹⁷ a broad spectrum of transition-metal complexes bearing these ligands has been investigated,^{17–25} including ruthenium(II) entities.^{23–25}

Recently, we reported on the syntheses of $[\text{Ru}(\text{bdmpza})\text{Cl}(\text{PPh}_3)_2]$ (**1a**) and $[\text{Ru}(\text{bpza})\text{Cl}(\text{PPh}_3)_2]$ (**1b**) (bpza, bis(pyrazol-1-yl)acetate; bdmpza, bis(3,5-dimethylpyrazol-1-yl)acetate (Figure 1)).²³ In particular, the sterically more hindered complex $[\text{Ru}(\text{bdmpza})\text{Cl}(\text{PPh}_3)_2]$ (**1a**) easily releases one of the two phosphine ligands and allows the substitution not only of a chloro but also of a triphenylphosphine ligand for κ^2 -coordinating carboxylato and 2-oxocarboxylato ligands.²⁵ In an effort to exploit the analogy between bis(pyrazol-1-yl)acetato and hy-

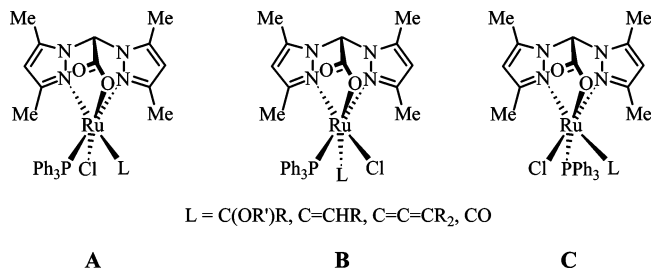


Figure 2. Possible structural isomers of ruthenium complexes $[\text{Ru}(\text{bdmpza})(\text{Cl})(\text{L})(\text{PPh}_3)]$.

dridotris(pyrazol-1-yl)borate (Tp) ligands, recent work in our laboratory has focused on organometallic complexes with the former ligands. Thus, here we report on neutral ruthenium carbene, vinylidene, and allenylidene complexes bearing the bdmpza ligand.

Results and Discussion

Three different structural isomers are conceivable for the carbene, vinylidene, allenylidene, and carbonyl complexes discussed in this report, which are (**A**) chloro ligand trans to carboxylate, (**B**) ligand L ($\text{L} = \text{C}(\text{OR}')\text{R}$, $\text{C}=\text{CHR}$, $\text{C}=\text{C}=\text{CR}_2$, CO) trans to carboxylate, and (**C**) phosphine trans to carboxylate (Figure 2).

Due to the trans influence of the pyrazole acceptor ligands, coordination of the phosphine donor trans to the carboxylate is very unlikely. Furthermore, all the NOE experiments were performed for the carbene, vinylidene, and allenylidene complexes, which will be discussed later in detail, showed cross-peaks between the PPh_3 signals and the pyrazole signals. Therefore, the formation of isomer **C** can be excluded, so far. Both isomers **A** and **B** are racemic mixtures of two enantiomers. Because of the loss of C_s symmetry in these isomers, two different sets of NMR signals are expected for the two pyrazolyl groups. For isomers of types **A** and **B** the pyrazole group next to the remaining phosphine ligand will be marked by a prime (e.g. Me^{\prime}) throughout this text.

Synthesis of the Vinylidene Complexes $[\text{Ru}(\text{bdmpza})\text{Cl}(\text{C}=\text{CHR})(\text{PPh}_3)]$ ($\text{R} = \text{Ph}$, Tol, Pr, Bu; **2a–d).** The steric hindrance associated with the bis(3,5-dimethylpyrazol-1-yl)acetato ligand labilizes one of the PPh_3 ligands in **1a**. Recently, we reported for $[\text{Ru}(\text{bdmpza})\text{Cl}(\text{PPh}_3)_2]$ (**1a**), for example, the substitution not only of a chloro but also of a triphenylphosphine ligand for κ^2 -coordinating carboxylato and 2-oxocarboxylato ligands.²⁵ Due to this observation, the reaction conditions were chosen to be quite similar to those for the rather mild synthesis of the corresponding Tp vinylidene complexes $[\text{RuCl}\{\kappa^3\text{-HB}(\text{pz})_3\}(\text{C}=\text{CHR})(\text{PPh}_3)]$ ($\text{R} = \text{Ph}$, Tol).²⁴ Following this procedure, we succeeded in synthesizing the four neutral vinylidene complexes $[\text{Ru}(\text{bdmpza})\text{Cl}(\text{C}=\text{CHR})(\text{PPh}_3)]$ ($\text{R} = \text{Ph}$, Tol, Pr, Bu; **2a–d**). The reaction of $[\text{Ru}(\text{bdmpza})\text{Cl}(\text{PPh}_3)_2]$ (**1a**) with 5 equiv of phenylacetylene afforded the vinylidene complex $[\text{Ru}(\text{bdmpza})\text{Cl}(\text{C}=\text{CHPh})(\text{PPh}_3)]$ (**2a**) within 4 h (Scheme 1).

The formation of the vinylidene complex **2a** proceeds much more quickly compared to that of the corresponding Tp complex $[\text{RuCl}\{\kappa^3\text{-HB}(\text{pz})_3\}(\text{C}=\text{CHPh})(\text{PPh}_3)]$ (36 h according to the literature)⁴ and the synthesis of the analogous Cp* complex $[\text{Ru}(\eta^5\text{-C}_5\text{Me}_5)\text{Cl}(\text{C}=\text{CHPh})(\text{PPh}_3)]$, which was carried out under reflux conditions.²⁶ In a similar reaction of $[\text{Ru}(\text{bpza})-$

(16) Sanford, M. S.; Love, J. A.; Grubbs, R. H. *Organometallics* **2001**, *20*, 5314–5318.

(17) Otero, A.; Fernández-Baeza, J.; Tejada, J.; Antiñolo, A.; Carrillo-Hermosilla, F.; Díez-Barra, E.; Lara-Sánchez, A.; Fernández-López, M.; Lanfranchi, M.; Pellinghelli, M. A. *J. Chem. Soc., Dalton Trans.* **1999**, 3537–3539.

(18) Otero, A.; Fernández-Baeza, J.; Antiñolo, A.; Tejada, J.; Lara-Sánchez, A. *Dalton Trans.* **2004**, 1499–1510.

(19) (a) Otero, A.; Fernández-Baeza, J.; Tejada, J.; Antiñolo, A.; Carrillo-Hermosilla, F.; Díez-Barra, E.; Lara-Sánchez, A.; Fernández-López, M. *Dalton Trans.* **2000**, 2367–2374. (b) Otero, A.; Fernández-Baeza, J.; Antiñolo, A.; Carrillo-Hermosilla, F.; Tejada, J.; Díez-Barra, E.; Lara-Sánchez, A.; Sánchez-Barba, L.; López-Solera, I. *Organometallics* **2001**, *20*, 2428–2430. (c) Otero, A.; Fernández-Baeza, J.; Antiñolo, A.; Carrillo-Hermosilla, F.; Tejada, J.; Lara-Sánchez, A.; Sánchez-Barba, L.; Fernández-López, M.; Rodríguez, A. M.; López-Solera, I. *Inorg. Chem.* **2002**, *41*, 5193–5202. (d) Otero, A.; Fernández-Baeza, J.; Antiñolo, A.; Tejada, J.; Lara-Sánchez, A.; Sánchez-Barba, L.; Rodríguez, A. M. *Eur. J. Inorg. Chem.* **2004**, 260–266. (e) Otero, A.; Fernández-Baeza, J.; Antiñolo, A.; Tejada, J.; Lara-Sánchez, A.; Sánchez-Barba, L.; Fernández-López, M.; López-Solera, I. *Inorg. Chem.* **2004**, *43*, 1350–1358.

(20) (a) Burzlaff, N.; Hegelmann, I.; Weibert, B. *J. Organomet. Chem.* **2001**, *626*, 16–23. (b) Burzlaff, N.; Hegelmann, I. *Inorg. Chim. Acta* **2002**, *329*, 147–150.

(21) (a) Beck, A.; Weibert, B.; Burzlaff, N. *Eur. J. Inorg. Chem.* **2001**, 521–527. (b) Hegelmann, I.; Beck, A.; Eichhorn, C.; Weibert, B.; Burzlaff, N. *Eur. J. Inorg. Chem.* **2003**, 339–347.

(22) Beck, A.; Barth, A.; Hübner, E.; Burzlaff, N. *Inorg. Chem.* **2003**, *42*, 7182–7188.

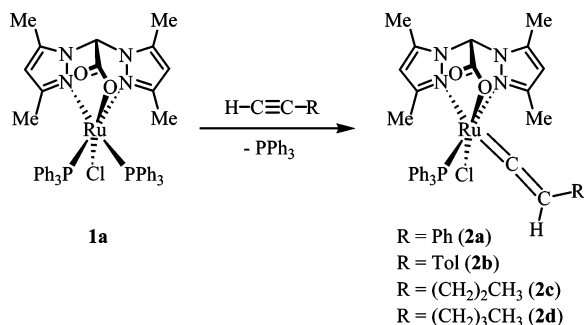
(23) López Hernández, A.; Müller, R.; Kopf, H.; Burzlaff, N. *Eur. J. Inorg. Chem.* **2002**, 671–677.

(24) (a) Hegelmann, I.; Burzlaff, N. *Eur. J. Inorg. Chem.* **2003**, 409–411. (b) Peters, L.; Burzlaff, N. *Polyhedron* **2004**, *23*, 245–251. (c) Ortiz, M.; Díaz, A.; Cao, R.; Otero, A.; Fernández-Baeza, J. *Inorg. Chim. Acta* **2004**, *357*, 19–24. (d) Ortiz, M.; Díaz, A.; Cao, R.; Suardíaz, R.; Otero, A.; Antiñolo, A.; Fernández-Baeza, J. *Eur. J. Inorg. Chem.* **2004**, 3353–3357.

(25) Müller, R.; Hübner, E.; Burzlaff, N. *Eur. J. Inorg. Chem.* **2004**, 2151–2159.

(26) Bruce, M. I.; Hall, B. C.; Zaitseva, N. N.; Skelton, B. W.; White, A. H. *J. Chem. Soc., Dalton Trans.* **1998**, 1793–1803.

Scheme 1. Syntheses of the Ruthenium Vinylidene Complexes 2a–d



$\text{Cl}(\text{PPh}_3)_2$ (**1b**) with phenylacetylene, we observed no formation of a vinylidene complex. Since $[\text{Ru}(\text{bpza})\text{Cl}(\text{PPh}_3)_2]$ (**1b**) is almost identical with $[\text{Ru}(\text{bdmpza})\text{Cl}(\text{PPh}_3)_2]$ (**1a**) in its electronic properties, but less bulky, we assume that this rather fast substitution reaction in **1a** is mainly due to steric reasons.

For practical reasons only a slight excess of 2 equiv of phenylacetylene in a THF suspension of $[\text{Ru}(\text{bdmpza})\text{Cl}(\text{PPh}_3)_2]$ (**1a**) proved also to be suitable for the synthesis of $[\text{Ru}(\text{bdmpza})\text{Cl}(\text{=C=CHPh})(\text{PPh}_3)]$ (**2a**), though longer reaction times were needed. The progress of the reaction can be monitored by IR spectroscopy of the THF reaction mixture, since the asymmetric carboxylate vibration of the tripodald bdm pza ligand shifts from 1672 cm^{-1} for **1a** to 1678 cm^{-1} for the product **2a**. The vinylidene complex **2a** shows the typical β -H NMR resonance of the vinylidene ligand at 4.93 ppm, splitted by a coupling $^4J_{\text{HP}}$ of 4.9 Hz. In the ^1H and $^{13}\text{C}\{^1\text{H}\}$ NMR spectra two different sets of signals were observed for the pyrazolyl groups of the bdm pza ligand. The vinylidene complex $[\text{Ru}(\text{bdmpza})\text{Cl}(\text{=C=CHTol})(\text{PPh}_3)]$ (**2b**) can be prepared in the same way by reaction of **1a** with *p*-tolylacetylene (Scheme 1). Two-dimensional NMR spectroscopy was applied for the signal assignment of **2b**. Most ^1H and $^{13}\text{C}\{^1\text{H}\}$ NMR signals of **2a** have been assigned in analogy to those of **2b**. In a ROESY experiment with **2b** cross-peaks were detected between the proton resonances (in ppm) at 1.89 (Me^3) and 7.73 (*o*- PPh_3), at 2.40 (Me^3) and 6.63 (*o*-Tol), and at 4.89 (H_β) and 7.73 (*o*- PPh_3). A weak NOE signal between 2.40 (Me^3) and 4.89 (H_β), but no signal between 1.89 (Me^3) and 6.63 (*o*-Tol), can be found as well. These data indicate a coordination of the vinylidene ligand *trans* to a pyrazolyl ring of the bdm pza ligand and thus indicate a type **A** isomer (see Figure 2). No rotation around the $\text{Ru}-\text{C}_\alpha$ and $\text{C}_\alpha-\text{C}_\beta$ bonds of the vinylidene ligand was observed, although a very fast rotation cannot be excluded, so far.^{27,28} Thus, the β -proton of the vinylidene ligand is oriented toward the PPh_3 ligand. The $^{13}\text{C}\{^1\text{H}\}$ NMR resonances of the β -carbons (**2a**, 113.1 ppm, **2b**, 115.1 ppm) are assigned by HMQC experiments and exhibit no J_{CP} coupling. However, the $^{13}\text{C}\{^1\text{H}\}$ NMR resonances of the α -C are found at 369.3 (**2a**) and 364.2 ppm (**2b**) with $^2J_{\text{CP}}$ couplings of 24.0 (**2a**) and 24.4 Hz (**2b**), respectively. These values are in good agreement with those of the vinylidene complex $[\text{RuCl}\{\kappa^3\text{-HB}(\text{pz})_3\}(\text{=C=CHTol})(\text{PPh}_3)]$ ($^{13}\text{C}\{^1\text{H}\}$ NMR: 370 (d, $^2J_{\text{CP}} = 19.4 \text{ Hz}$, C_α), 112 (C_β) ppm) reported by Hill et al.⁴

Although the crude reaction mixtures showed the formation of traces of second products, which are probably traces of structural type **B** isomers, only single type **A** isomers were

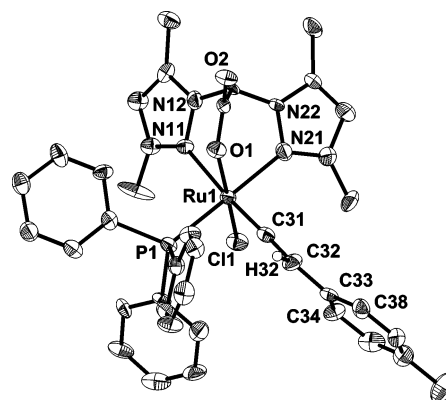


Figure 3. Molecular structure of $[\text{Ru}(\text{bdmpza})\text{Cl}(\text{=C=CHTol})(\text{PPh}_3)]$ (**2b**) with thermal ellipsoids drawn at the 50% probability level. Most hydrogen atoms and solvent molecules are omitted for clarity.

Table 1. Selected Bond Lengths (Å) and Angles (deg) of Complex 2b

Ru–N(11)	2.257(10)	Ru–C(31)	1.821(13)
Ru–N(21)	2.176(10)	C(31)–C(32)	1.347(18)
Ru–O(1)	2.104(9)	C(32)–H(32)	0.93(12)
Ru–P	2.338(3)	C(32)–C(33)	1.474(18)
Ru–Cl	2.396(3)		
N(11)–Ru–N(21)	82.6(4)	O(1)–Ru–Cl	170.9(2)
O(1)–Ru–N(11)	82.5(3)	N(21)–Ru–P	176.4(3)
O(1)–Ru–N(21)	85.6(4)	N(11)–Ru–C(31)	175.8(5)
O(1)–Ru–P	91.3(2)	C(33)–C(32)–H(3)	133(7)
P–Ru–Cl	92.61(12)	Cl–Ru–C(31)	93.2(4)
P–Ru–C(31)	84.9(4)	Ru–C(31)–C(32)	176.7(11)
P–Ru–C(32)–C(33)			114.4(11)
C(31)–C(32)–C(33)–C(34)			–18(2)

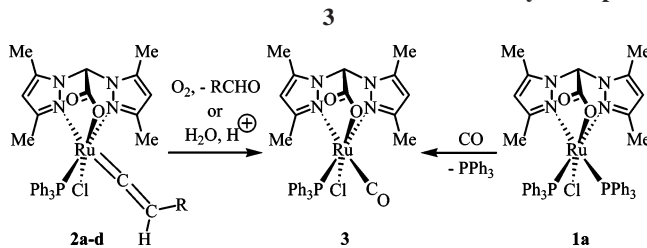
isolated after workup in the case of **2a,b**. In addition to the spectroscopic evidence, which has been discussed above, this type **A** configuration is backed up also by an X-ray structure determination of the vinylidene complex $[\text{Ru}(\text{bdmpza})\text{Cl}(\text{=C=CHTol})(\text{PPh}_3)]$ (**2b**) (Figure 3, Table 1). Therefore, the molecular structure of **2b** exhibits a type **A** configuration with the vinylidene ligand *trans* to one of the pyrazolyl groups and the chloro ligand *trans* to the carboxylate donor of the bdm pza ligand (Figure 3).

The molecular structure of **2b** is almost identical with those of the analogous Tp and Cp* complexes $[\text{RuCl}\{\kappa^3\text{-HB}(\text{pz})_3\}(\text{=C=CHPh})(\text{PPh}_3)]$ and $[\text{Ru}(\eta^5\text{-C}_5\text{Me}_5)\text{Cl}(\text{=C=CHPh})(\text{PPh}_3)]$,^{2,26} apart from the more complicated configuration issue described above. Complex **2b** exhibits an almost octahedral coordination geometry of ruthenium. The length of the $\text{Ru}=\text{C}_\alpha$ bond at $\text{Ru}-\text{C}(31) = 1.821(13) \text{ \AA}$ is comparable to those in other neutral vinylidene ruthenium complexes.^{2,26} The vinylidene unit $\text{Ru}=\text{C}_\alpha=\text{C}_\beta$ with the bond angle $\text{Ru}-\text{C}(31)-\text{C}(32) = 176.7(11)^\circ$ is essentially linear. The $\text{C}_\alpha=\text{C}_\beta$ bond length of $1.348(6) \text{ \AA}$ is slightly longer than expected for a $\text{C}(\text{sp})=\text{C}(\text{sp}^2)$ double bond, but a similar distance has also been observed for the Cp* complex. The torsion angle $\angle \text{C}(31)-\text{C}(32)-\text{C}(33)-\text{C}(34)$ of $-18(2)^\circ$ indicates a conjugation of the vinylidene π system with the aromatic substituent. The sum of bond angles between the three facial binding chloro, PPh_3 , and vinylidene ligands with $\sum_{\text{facial}} = 92.61(12)^\circ + 84.9(4)^\circ + 93.2(4)^\circ = 270.7^\circ$ is rather small compared to corresponding values of $[\text{RuCl}\{\kappa^3\text{-HB}(\text{pz})_3\}(\text{=C=CHPh})(\text{PPh}_3)]$ ($\sum_{\text{facial}} = 282.32^\circ$) and $[\text{Ru}(\eta^5\text{-C}_5\text{Me}_5)\text{Cl}(\text{=C=CHPh})(\text{PPh}_3)]$ ($\sum_{\text{facial}} = 278.2^\circ$). This might be caused by the bdm pza ligand being more bulky than the Cp* or Tp ligand. Thus, substitution of a bulky PPh_3 ligand for a

(27) Hansen, H. D.; Nelson, J. H. *Organometallics* **2000**, *19*, 4740–4755.

(28) Urtel, K.; Frick, A.; Huttner, G.; Zsolnai, L.; Kircher, P.; Rutsch, P.; Kaifer, E.; Jacobi, A. *Eur. J. Inorg. Chem.* **2000**, 33–50.

Scheme 2. Formation of the Ruthenium Carbonyl Complex 3



vinylidene ligand eases the steric situation, causing a much faster reaction with the bdpmpza complex than with the Tp and Cp* complexes.

In addition to the aromatic vinylidene complexes, also alkyl vinylidene complexes have been synthesized (Scheme 1). By the same procedure given above, using 1-pentyne or 1-hexyne, the corresponding vinylidene complexes [Ru(bdpmpza)Cl(=C=CHPr)(PPh₃)] (**2c**) and [Ru(bdpmpza)Cl(=C=CHBu)(PPh₃)] (**2d**) have been isolated. IR and NMR spectroscopic data of **2c,d** are quite similar to those of **2a,b**. Again only one major isomer was isolated in the case of [Ru(bdpmpza)Cl(=C=CHPr)(PPh₃)] (**2c**). The crude reaction mixture showed both isomers. For [Ru(bdpmpza)Cl(=C=CHBu)(PPh₃)] (**2d**) an approximately 50:50 ratio of the two isomers was found in the isolated product. The reason for this might be the rather different solubility of complex **2d** compared to those of **2a–c**. Whereas the vinylidene complexes **2a–c** precipitated directly from the reaction mixture, pentane had to be used to precipitate **2d**. Thus, in the case of the complexes **2a–c** the reaction equilibrium might be drawn to the less soluble isomer.

The complexes [Ru(bdpmpza)Cl(=C=CHPr)(PPh₃)] (**2c**) and [Ru(bdpmpza)Cl(=C=CHBu)(PPh₃)] (**2d**) are less stable toward oxygen compared to the case for the complexes **2a,b**. This is reasonable, due to the missing stabilization of the vinylidene moiety by the conjugated π system.

During several attempts to crystallize the vinylidene complexes **2a–d** the formation of the carbonyl complex [Ru(bdpmpza)Cl(CO)(PPh₃)] (**3**) was occasionally observed. **3** can also be obtained in a direct synthesis by replacing a PPh₃ ligand of [Ru(bdpmpza)Cl(PPh₃)₂] (**1a**) with CO (Scheme 2). Similar syntheses carried out by replacing vinylidene ligands with CO have recently been reported for Tp carbonyl complexes such as [RuCl(κ^3 -HB(pz)₃)(CO)(PPh₃)].⁸ Exposing a solution of **1a** to CO thus produces an identical sample of **3** and proves the formation of the carbonyl complex **3** by degradation of the vinylidene complexes **2a–d** as stated above. The identities of the two samples of **3** were proven by ¹H NMR and IR spectroscopy. Mass spectrometric data with peaks at *m/z* 674 [M⁺], 646 [M⁺ – CO], and 639 [M⁺ – Cl] revealed the formation of the carbonyl complex **3**. An IR signal at 1969 cm⁻¹ (CH₂Cl₂) and a doublet in the ¹³C{¹H} NMR spectrum at 202.6 ppm (²*J*_{CP} = 19.8 Hz) can be assigned to the carbonyl ligand. These values correspond well to those reported for [RuCl(κ^3 -HB(pz)₃)(CO)(PPh₃)] (IR (Nujol) 1965 cm⁻¹; ¹³C{¹H} NMR 203.5 ppm (²*J*_{CP} = 16 Hz))²⁹ and for the acetato complex [Ru(bdpmpza)(O₂CCH₃)(CO)(PPh₃)] (IR (CH₂Cl₂) 1977 cm⁻¹; ¹³C{¹H} NMR 205.3 ppm (²*J*_{CP} = 19.8 Hz)), which we obtained recently.³⁰

Similar degradation reactions of ruthenium vinylidene complexes, either neutral or cationic, to form ruthenium carbonyl complexes have been reported by various authors before. In

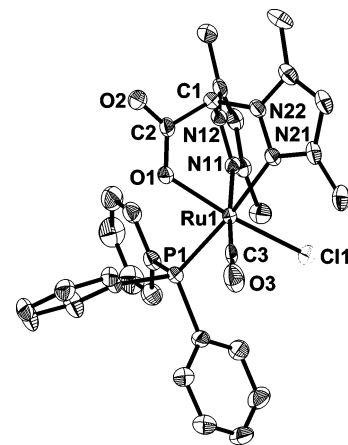


Figure 4. Molecular structure of [Ru(bdpmpza)Cl(CO)(PPh₃)] (**3**) with thermal ellipsoids drawn at the 50% probability level. Hydrogen atoms and solvent molecules are omitted for clarity.

these literature cases a reaction either with dioxygen^{5,31,32} or with H₂O takes place.^{33–35} Both conditions are quite conceivable for some of our long-term crystal-growing experiments. To distinguish between these two possible pathways, 5 equiv of water were added to a sample of [Ru(bdpmpza)Cl(=C=CHPh)(PPh₃)] (**2a**). The reaction mixture was monitored by the IR signal at 1969 cm⁻¹ (CH₂Cl₂). After 24 h under anaerobic conditions no formation of **3** was observed. Once the mixture was exposed to air, formation of the carbonyl complex [Ru(bdpmpza)Cl(CO)(PPh₃)] (**3**) was observed within 3 h.

The hypothesis of an oxidative cleavage of the C=C bond (Scheme 2) is also supported by the observation of benzaldehyde in the reaction mixture with a ¹H NMR signal of the HC=O group at 9.94 ppm.

Nevertheless, for a mixture of [Ru(bdpmpza)Cl(=C=CHPh)(PPh₃)] (**2a**) with a 30-fold excess of water in CDCl₃ we detected also the formation of the carbonyl complex **3** under acidic conditions (~3 equiv of HCl) within a few days. Surprisingly, during this reaction no toluene is formed, but we observed the formation of an intermediate complex with a singlet at 13.31 ppm and an AB system (4.48 and 3.53 ppm, *J*_{AB} = 14.4 Hz) in the ¹H NMR spectrum. These signals might be assigned to a =C(OH) group and a benzyl group and seem to indicate the intermediate hydroxycarbene complex [Ru(bdpmpza)Cl(=C(OH)-CH₂Ph)(PPh₃)]. Further acid-induced reactivity studies with the vinylidene complexes are currently investigated.

Thus, both degradation pathways, oxidative cleavage of the C=C bond with O₂ and an acid-induced addition of H₂O, are possible for the vinylidene complexes **2a–d**.

In an attempt to crystallize the vinylidene complex **2b** from CH₂Cl₂/diethyl ether, crystals of the carbonyl complex [Ru(bdpmpza)Cl(CO)(PPh₃)] (**3**) suitable for an X-ray structure determination were obtained. The molecular structure (Figure 4, Table 2) reveals the formation of the carbonyl complex **3**. The C(3)–O(3) and Ru–C(3) bond distances of the carbonyl ligand in **3** at 1.151(6) and 1.821(5) Å are in the expected range for other ruthenium carbonyl complexes. Similar Tp ruthenium

(31) Bianchini, C.; Innocenti, P.; Peruzzini, M.; Romerosa, A.; Zanolini, F. *Organometallics* **1996**, *15*, 272–285.

(32) Pavlik, S.; Schmid, R.; Kirchner, K.; Mereiter, K. *Monatsh. Chem.* **2004**, *135*, 1349–1357.

(33) Barthel-Rosa, L. P.; Maitra, K.; Fischer, J.; Nelson, J. H. *Organometallics* **1997**, *16*, 1714–1723.

(34) Bianchini, C.; Casares, J. A.; Peruzzini, M.; Romerosa, A.; Zanolini, F. *J. Am. Chem. Soc.* **1996**, *118*, 4585–4594.

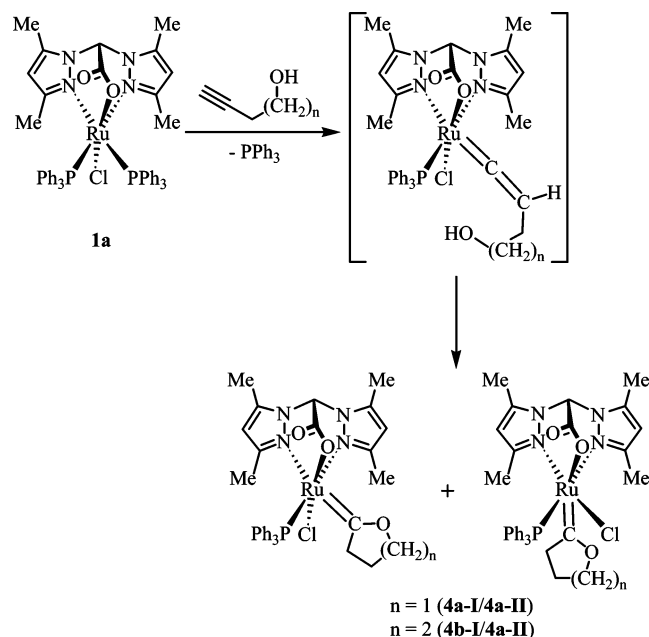
(35) Jiménez-Tenorio, M.; Palacios, M. D.; Puerta, M. C.; Valerga, P. *J. Organomet. Chem.* **2004**, *689*, 2853–2859.

(29) Sun, N.-Y.; Simpson, S. J. *J. Organomet. Chem.* **1992**, *434*, 341–349.

(30) Müller, R.; Hübner, E.; Burzlaff, N. Manuscript in preparation.

Table 2. Selected Bond Lengths (Å) and Angles (deg) of the Carbonyl Complex 3

Ru–N(11)	2.184(4)	Ru–Cl	2.3964(13)
Ru–N(21)	2.158(4)	Ru–C(3)	1.821(5)
Ru–O(1)	2.096(3)	C(3)–O(3)	1.151(6)
Ru–P	2.3266(13)		
N(11)–Ru–N(21)	82.78(14)	O(1)–Ru–Cl	174.48(9)
O(1)–Ru–N(11)	86.20(13)	N(21)–Ru–P	173.88(10)
O(1)–Ru–N(21)	86.12(13)	N(11)–Ru–C(3)	174.47(17)
O(1)–Ru–P	87.76(9)	Cl–Ru–C(3)	88.83(15)
P–Ru–Cl	96.59(5)	Ru–C(3)–O(3)	178.0(4)
P–Ru–C(3)	88.46(14)		

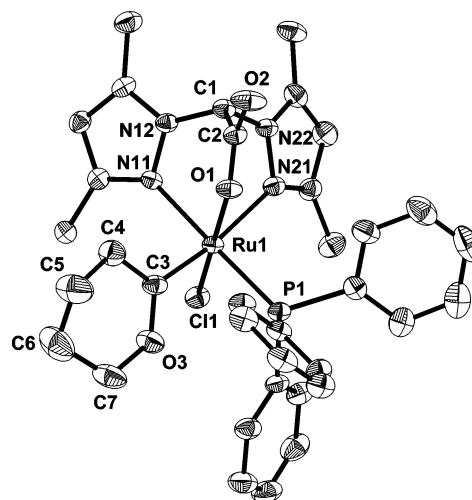
Scheme 3. Syntheses of the Ruthenium Carbene Complexes 4a,b

carbonyl complexes show molecular structures with 1.137(8) and 1.848(6) Å for $[\text{RuCl}\{\kappa^3\text{-HB}(\text{pz})_3\}(\text{CO})(\text{PPh}_3)]$, 1.102(4) and 1.863(4) Å for $[\text{RuCl}\{\kappa^3\text{-HB}(\text{pz})_3\}(\text{CO})\{\text{PiPr}(\text{Ph})_2\}]$, and 1.099(2) and 1.868(2) Å for $[\text{RuCl}\{\kappa^3\text{-HB}(\text{pz})_3\}(\text{CO})(\kappa^1\text{-P-Ph}_2\text{PCH}_2\text{CH}_2\text{OMe})]$.^{5,8,32}

Synthesis of the Cyclic Fischer Carbene Complexes

$[\text{Ru}(\text{bdmpza})\text{Cl}(\text{C}(\text{CH}_2)_{n+2}\text{O})(\text{PPh}_3)]$ ($n = 1, 2$; **4a,b**). A similar reaction of $[\text{Ru}(\text{bdmpza})\text{Cl}(\text{PPh}_3)_2]$ (**1a**) with terminal alkynols, e.g. 3-butyne-1-ol and 4-pentyne-1-ol, results in the formation of the cyclic, heteroatom-stabilized Fischer carbene complexes $[\text{Ru}(\text{bdmpza})\text{Cl}(\text{C}(\text{CH}_2)_{n+2}\text{O})(\text{PPh}_3)]$ ($n = 1, 2$; **4a,b**) (Scheme 3).

The formation of cyclic Fischer carbene complexes by ruthenium-mediated activation of 3-butyne-1-ol and 4-pentyne-1-ol has been reported before to make close analogues of **4a,b**.^{27,33,36–42} Other routes to ruthenium complexes with $\text{C}(\text{CH}_2)_{n+2}\text{O}$ moieties via ruthenium allenylidene and vinyl-

**Figure 5.** Molecular structure of $[\text{Ru}(\text{bdmpza})\text{Cl}(\text{C}(\text{CH}_2)_4\text{O})(\text{PPh}_3)]$ (**4b-I**) with thermal ellipsoids drawn at the 50% probability level. Hydrogen atoms are omitted for clarity.

idene complexes are also well-known.^{43–45} Obviously, in the syntheses with terminal alkynols the first intermediates are the vinylidene complexes $[\text{Ru}(\text{bdmpza})\text{Cl}(\text{C}=\text{CH}(\text{CH}_2)_{n+1}\text{OH})(\text{PPh}_3)]$ ($n = 1, 2$), which then react further via an intramolecular addition of the alcohol functionality to the α -carbon (Scheme 3) to form the cyclic Fischer carbene complexes **4a,b**.

However, in none of our experiments were these intermediate vinylidene complexes observed or isolated, although this has been reported for similar cationic vinylidene complexes such as $[\text{Ru}(\eta^5\text{-C}_5\text{Me}_5)(\text{C}=\text{CHCH}_2\text{OH})(\text{PR}_3)_2]\text{PF}_6$ ($\text{PR}_3 = \text{DPVP} = \text{diphenylvinylphosphine}$).³³ The intramolecular alcohol addition results in cyclic carbene complexes with a five-membered ring in case of the reaction with but-3-yn-1-ol and with a six-membered ring in the case of pent-4-yn-1-ol. For both products **4a,b** two isomers are found for each, **4a-I/4a-II** and **4b-I/4b-II**, which are according to two-dimensional NMR experiments most likely structural isomers of types **A** and **B** (Figure 2, Scheme 3). Due to the chirality at the metal center the ring CH_2 protons are diastereotopic. This causes rather complicated ^1H NMR spectra with several multiplet signals in the aliphatic region between 1.47 and 4.66 ppm in the case of **4a** and 1.24 and 4.47 ppm in the case of **4b**, similar to what is reported for other cyclic oxycarbene complexes.^{27,37} Two-dimensional NMR methods were used to analyze and assign these protons. A crystal of **4b-I** suitable for a structure determination was obtained from THF. The molecular structure shows a type **A** isomer with the carbene ligand and the triphenylphosphine ligand in the two positions trans to the pyrazoles, while the chloro ligand occupies the position trans to the carboxylate donor (Figure 5, Table 3). It is noteworthy that almost all cyclic ruthenium Fischer carbene complexes in the literature so far are cationic complexes, except for one very recent example.⁴² Furthermore, most of the former examples bear either a chelating bis-phosphine ligand or two phosphine ligands. Well suited for a structural comparison with the complexes $[\text{Ru}(\text{bdmpza})\text{Cl}(\text{C}(\text{CH}_2)_{n+2}\text{O})(\text{PPh}_3)]$ ($n = 1,$

(36) Dötz, K. H.; Sturm, W.; Alt, H. G. *Organometallics* **1987**, *6*, 1424–1427.

(37) Le Bozec, H.; Ouzzine, K.; Dixneuf, P. H. *Organometallics* **1991**, *10*, 2768–2772.

(38) Beddoes, R. L.; Grime, R. W.; Hussain, Z. I.; Whiteley, M. W. J. *Organomet. Chem.* **1996**, *526*, 371–378.

(39) Leung, W.-H.; Chan, E. Y. Y.; Williams, I. D.; Wong, W.-T. *Organometallics* **1997**, *16*, 3234–3240.

(40) Barthel-Rosa, L. P.; Maitra, K.; Nelson, J. H. *Inorg. Chem.* **1998**, *37*, 633–639.

(41) Keller, A.; Jasionka, B.; Glowiak, T.; Ershov, A.; Matusiak, R. *Inorg. Chim. Acta* **2003**, *344*, 49–60.

(42) Pavlik, S.; Mereiter, K.; Puchberger, M.; Kirchner, K. J. *Organomet. Chem.* **2005**, *690*, 5497–5507.

(43) Esteruelas, M. A.; Gómez, A. V.; López, A. M.; Oliván, M.; Oñate, E.; Ruiz, N. *Organometallics* **2000**, *19*, 4–14.

(44) Nombel, P.; Lugan, N.; Mathieu, R. J. *Organomet. Chem.* **1995**, *503*, C22–C25.

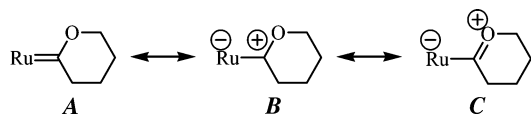
(45) Chang, C.-W.; Lin, Y.-C.; Lee, G.-H.; Wang, Y. *Organometallics* **2000**, *19*, 3211–3219.

Table 3. Selected Bond Lengths (Å) and Angles (deg) of the Carbene Complex **4b-I**

Ru–N(11)	2.156(3)	Ru–Cl	2.3861(11)
Ru–N(21)	2.269(3)	Ru–C(3)	1.918(4)
Ru–O(1)	2.115(2)	C(3)–O(3)	1.323(4)
Ru–P	2.3107(11)	C(3)–C(4)	1.516(5)
N(11)–Ru–N(21)	81.88(10)	O(1)–Ru–Cl	173.01(6)
O(1)–Ru–N(11)	84.85(9)	N(21)–Ru–P	97.88(7)
O(1)–Ru–N(21)	84.58(9)	N(11)–Ru–C(3)	91.31(12)
O(1)–Ru–P	93.21(6)	Cl–Ru–C(3)	94.17(10)
P–Ru–Cl	90.70(3)	Ru–C(3)–O(3)	121.7(3)
P–Ru–C(3)	88.81(10)	Ru–C(3)–C(4)	120.9(2)

2; **4a,b**) are the complexes $[\text{RuCl}(\eta^6\text{-C}_6\text{Me}_6)(=\text{C}(\text{CH}_2)_3\text{O})\text{-}(\text{DPVP})\text{PF}_6$ and $[\text{RuCl}\{\kappa^3\text{-HB}(\text{pz})_3\}(\text{C}(\text{CH}_2)_3\text{O})(\text{PPh}_3)]$, which exhibit rather similar Ru–carbene distances of 1.958(7) and 1.921(2) Å, respectively.^{27,42} The distances Ru–C(3) = 1.918(4) Å, C(3)–O(3) = 1.323(4) Å, and C(3)–C(4) = 1.516(5) Å of the cyclic oxycarbene ligand ($=\text{C}(\text{CH}_2)_4\text{O}$) in **4b-I** also agree well with those reported for the complex $[\text{Ru}(\eta^5\text{-C}_5\text{H}_5)(=\text{C}(\text{CH}_2)_4\text{O})(\text{dppe})\text{PF}_6$ (dppe = $\text{Ph}_2\text{PCH}_2\text{CH}_2\text{PPh}_2$) (Ru–C = 1.938(4) Å; C–O = 1.314(5) Å, C–C = 1.497(6) Å).³⁸

Three canonical representations (**A–C**) can be drawn for the Fischer-type oxycarbene complexes $[\text{Ru}(\text{bdmpza})(\text{Cl})(=\text{C}(\text{CH}_2)_3\text{O})(\text{PPh}_3)]$ (**4a**) and $[\text{Ru}(\text{bdmpza})(\text{Cl})(=\text{C}(\text{CH}_2)_4\text{O})(\text{PPh}_3)]$ (**4b**), of which **B** and **C** suggest free rotation about a Ru–C single bond.²⁷



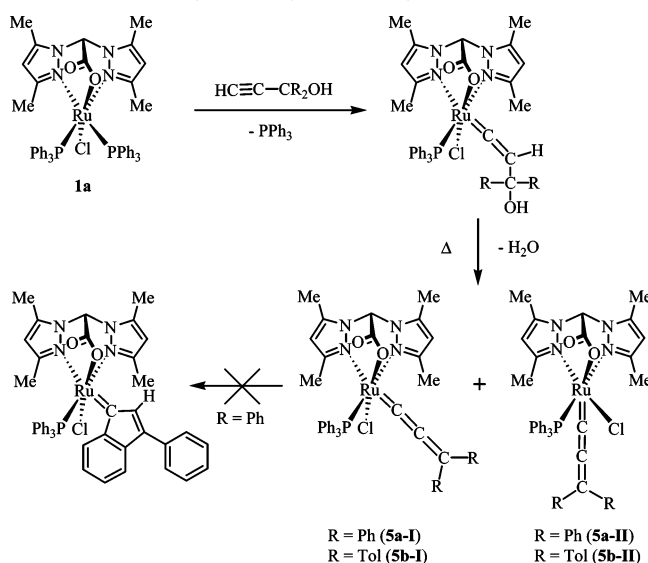
Thus, contributions of form **B** and **C** cause us to expect a low rotational barrier for complexes **4a,b** and make the rather long Ru–C_α distance plausible. The plane O(3)–C(3)–C(4) in the molecular structure of **4b** deviates from the plane N(11)–N(21)–P(1)–Ru(1) by approximately 45°.

The pentacyclic oxycarbene ligands of both isomers of **4a** are evidenced in the ¹³C{¹H} NMR spectra by the resonances at 311.9 ppm (²J_{CP} = 16.6 Hz) (**4a-I**, isomer A) and 311.1 ppm (²J_{CP} = 14.3 Hz) (**4a-II**, isomer B) for the carbene carbon atoms. The CH₂ carbon resonances are observed at 22.2 (**4a-I**), 23.5 (**4a-II**), 52.3 (**4a-I**), 51.3 (**4a-II**), 81.1 (**4a-I**), and 79.5 ppm (**4a-II**), respectively. Related pentacyclic oxycarbene complexes exhibit these resonances at 317.38 (²J_{CP} = 22.0 Hz), 21.54,

55.96, and 87.98 ppm for $[\text{RuCl}(\eta^6\text{-C}_6\text{Me}_6)(=\text{C}(\text{CH}_2)_3\text{O})\text{-}(\text{PMe}_3)\text{PF}_6$, at 313.25 (²J_{CP} = 14.0 Hz), 21.13, 55.78, and 88.58

ppm for $[\text{RuCl}(\eta^6\text{-C}_6\text{Me}_6)(=\text{C}(\text{CH}_2)_3\text{O})(\text{DPVP})\text{PF}_6$, and at 314.4 (²J_{CP} = 13.8 Hz), 22.7, 54.3, and 80.8 ppm for $[\text{RuCl}\{\kappa^3\text{-HB}(\text{pz})_3\}(\text{C}(\text{CH}_2)_3\text{O})(\text{PPh}_3)]$.^{27,37,42} Also, the ¹³C{¹H} NMR data of **4b** are consistent with a hexacyclic oxycarbene ligand with resonances at 18.1 (**4b-I**, isomer A), 17.3 (**4b-II**, isomer B), 22.2 (**4b-I**), 21.9 (**4b-II**), 46.5 (**4b-I**), 46.9 (**4b-II**), 73.7 (**4b-I**), 72.1 (**4b-II**), 315.7 (**4b-I**) (d, ²J_{CP} = 16.1 Hz), and 314.5 ppm (**4b-II**) (²J_{CP} not resolved). This coincides well with the resonances reported for the hexacyclic oxycarbene complexes

$[\text{Ru}(\eta^5\text{-C}_5\text{H}_5)(=\text{C}(\text{CH}_2)_4\text{O})(\text{dppe})\text{PF}_6$ at 17.4, 21.2, 54.0, 73.6, and 304.4 ppm (t, ²J_{CP} = 12.6 Hz) as well as for $[\text{RuCl}\{\kappa^3\text{-HB}(\text{pz})_3\}(\text{C}(\text{CH}_2)_4\text{O})(\text{PPh}_3)]$ at 16.7, 22.0, 48.2,

Scheme 4. Formation of the Ruthenium Allenylidene Complexes $[\text{Ru}(\text{bdmpza})(\text{Cl})(=\text{C}=\text{C}=\text{CR}_2)(\text{PPh}_3)]$ (**5a-I/5a-II**, R = Ph; **5b-I/5b-II**, R = Tol)

71.7, and 320.2 ppm (²J_{CP} = 13.8 Hz).^{38,42} Finally it is noted that the yellow color of the cyclic oxycarbene complexes **4a,b** differs from the green color which we observed recently for the ruthenium benzylidene complexes $[\text{Ru}(\text{bdmpza})\text{Cl}(\text{PCy}_3)(=\text{CHPh})]$ and $[\text{Ru}(\text{bpza})\text{Cl}(\text{PCy}_3)(=\text{CHPh})]$ but matches with $[\text{RuCl}(\eta^6\text{-C}_6\text{Me}_6)(=\text{C}(\text{CH}_2)_3\text{O})(\text{DPVP})\text{PF}_6$, which is yellow as well.^{27,46}

Synthesis of the Allenylidene Complexes $[\text{Ru}(\text{bdmpza})\text{-Cl}(\text{C}=\text{C}=\text{CR}_2)(\text{PPh}_3)]$ (R = Ph, Tol; **5a,b).** The preparation of allenylidene complexes was carried out by using an excess of propargylic alcohol as the terminal alkyne, similar to the method of Selegue.⁴⁷ The reaction of $[\text{RuCl}\{\kappa^3\text{-HB}(\text{pz})_3\}(\text{PPh}_3)_2]$ with $\text{HC}\equiv\text{C}-\text{CPh}_2\text{OH}$ has been previously reported by Hill and co-workers to provide the allenylidene complex $[\text{RuCl}\{\kappa^3\text{-HB}(\text{pz})_3\}(\text{C}=\text{C}=\text{CPh}_2)(\text{PPh}_3)]$.⁴⁹ To simplify the spectroscopic analysis, we used the propargylic alcohols $\text{HC}\equiv\text{CCR}_2\text{OH}$ (R = Ph, Tol) instead of the chiral alkynes $\text{HC}\equiv\text{CCR}^1\text{R}^2\text{OH}$. The formation of the allenylidene complexes $[\text{Ru}(\text{bdmpza})\text{Cl}(\text{C}=\text{C}=\text{CR}_2)(\text{PPh}_3)]$ (R = Ph, Tol; **5a,b**) via the intermediate vinylidene complexes $[\text{Ru}(\text{bdmpza})\text{Cl}(\text{C}=\text{C}=\text{CH}-\text{CR}_2\text{OH})(\text{PPh}_3)]$ is rather slow in THF at ambient temperature (Scheme 4) and takes usually more than 24 h to complete. Although no such vinylidene intermediates were isolated, these are clearly indicated during the reaction by the vinylidene β-H NMR signal at 4.71 ppm (⁴J_{HP} = 4.9 Hz) in the case of $\text{HC}\equiv\text{CCPh}_2\text{OH}$.

The vinylidene β-H ⁴J_{HP} couplings agree well with those of the vinylidene complexes **2a–d** discussed above. Similar vinylidene intermediates have been reported by other authors before.⁴⁸ The formation of the allenylidene complexes $[\text{Ru}(\text{bdmpza})\text{Cl}(\text{C}=\text{C}=\text{CR}_2)(\text{PPh}_3)]$ (R = Ph, Tol; **5a,b**) is indicated by a color change of the reaction mixture from yellow to purple and is completed by heating under reflux for 2–4 h. The allenylidene complex formation can be monitored by the disappearance of the vinylidene β-H ¹H NMR resonance. According to the ¹H, ¹³C{¹H}, and ³¹P{¹H} NMR spectra, two

(46) Kopf, H.; Hübner, E.; Pietraszuk, C.; Burzlaff, N. Manuscript in preparation.

(47) Selegue, J. P. *Organometallics* **1982**, *1*, 217–218.

(48) Braun, T.; Steinert, P.; Werner, H. *J. Organomet. Chem.* **1995**, *488*, 169–176.

isomers of the allenylidene complexes $[\text{Ru}(\text{bdmpza})(\text{Cl})(=\text{C}=\text{C}=\text{CR}_2)(\text{PPh}_3)]$ (**5a-I/5a-II**, R = Ph; **5b-I/5b-II**, R = Tol) are formed. The neutral allenylidene complexes are rather stable toward oxygen and water and can thus be purified by column chromatography under aerobic conditions. Furthermore, this allows also a separation of the isomers **5a-I/5a-II** (R = Ph) and **5b-I/5b-II** (R = Tol), of which the major isomers **5a-I** and **5b-I** exhibit a purple color and the minor isomers **5a-II** and **5b-II** show a red color. Two-dimensional NMR studies indicate that the violet isomers (**5a-I**, **5b-I**) are of type **A** and the red isomers (**5a-II**, **5b-II**) are of type **B**. The ratio of the isomers varies greatly, depending on reaction time and temperature. It is even possible to shift the ratio to the red isomers **5a-II** and **5b-II** by heating the reaction mixture in THF under reflux for 24 h.

Similar to the case for the vinylidene complexes **2a-d** the allenylidene complexes **5a-I/5a-II** and **5b-I/5b-II** exhibit $\nu_{\text{as}}(\text{CO}_2^-)$ signals between 1663 and 1669 cm^{-1} in the IR spectra. Thus, this $\nu_{\text{as}}(\text{CO}_2^-)$ signal of the bdmpza ligand is not useful to monitor the conversion of the intermediate vinylidene complexes $[\text{Ru}(\text{bdmpza})\text{Cl}(=\text{C}=\text{CH}-\text{CR}_2\text{OH})(\text{PPh}_3)]$ to the allenylidene complexes. Characteristic features for **5a-I/5a-II** and **5b-I/5b-II** are the strong $\text{C}=\text{C}=\text{C}$ stretches in the IR spectra around 1918 cm^{-1} . The $^{13}\text{C}\{^1\text{H}\}$ NMR signals of the allenylidene ligands have been assigned to 142.1 (C_γ), 227.4 (C_β), and 305.5 ppm (C_α , $^2J_{\text{CP}} = 26.4$ Hz) for the violet isomer **5a-I** and to 142.5 (C_γ), 220.0 (C_β), and 299.0 ppm (C_α , $^2J_{\text{CP}} = 26.1$ Hz) for the violet isomer **5b-I**. The $^{31}\text{P}\{^1\text{H}\}$ NMR signals of these violet isomers have been found at 37.3 (**5a-I**) and 38.1 ppm (**5b-I**). These values are very close to those of the type **A** isomers of the aryl-substituted vinylidene complexes (both (**2a,b**) 37.5 ppm). Thus, these data also indicate that **5a-I** and **5b-I** are type **A** isomers with the allenylidene ligand in a position trans to a pyrazole donor. The red type **B** isomers show $^{13}\text{C}\{^1\text{H}\}$ NMR allenylidene ligand signals at 149.2 (C_γ), 239.7 (C_β) and 314.7 ppm (C_α , $^2J_{\text{CP}} = 19.1$ Hz) (**5a-II**) and at 150.0 (C_γ), 232.8 (C_β) and 311.0 ppm (C_α , $^2J_{\text{CP}} = 18.8$ Hz) (**5b-II**), respectively. The $^{31}\text{P}\{^1\text{H}\}$ NMR signals of the red type **B** isomers have been found at 32.3 (**5a-II**) and 33.7 ppm (**5b-II**), which is again quite similar to those for the vinylidene complexes **2a,b** (32.3 and 32.6 ppm for the **B** type isomers). ROESY NMR spectra of **5a-II** and **5b-II** exhibit cross-peaks indicating a spatial proximity for the aryl ortho H atoms of the allenylidene ligand with both methyl groups Me^3 and $\text{Me}^{3'}$ of the bdmpza ligand. This is plausible for a coordination of the allenylidene ligand trans to the carboxylate donor. Two-dimensional NMR techniques (ROESY) were used to distinguish the bdmpza methyl groups Me^3 , $\text{Me}^{3'}$, Me^5 , and $\text{Me}^{5'}$ of the violet type **A** isomers **5a-I** and **5b-I**. This was also possible for the red type **B** isomers **5a-II** and **5b-II**, for which the ROESY spectra showed a spatial proximity of $\text{Me}^{3'}$ to the PPh_3 ligand. C,H-correlated NMR spectra (HMBC) of **5a-I/5a-II** revealed cross resonances at 7.57 and 142.1 ppm (**5a-I**) as well as at 7.69 and 149.2 ppm (**5a-II**), which were assigned to the $^3J_{\text{CH}}$ coupling of the phenyl ortho hydrogen atom with the allenylidene γ -carbon atom. This helped us not only to assign the γ -C signals in the $^{13}\text{C}\{^1\text{H}\}$ NMR spectra but also to exclude a rearrangement of the allenylidene complex to an indenylidene complex. Such a rearrangement has been reported recently in an attempt to obtain the related allenylidene complex $[\text{Ru}(\text{Cl})_2(\text{PPh}_3)_2(=\text{C}=\text{C}=\text{CPh}_2)]$.^{49,50} Finally, the structural proposals for

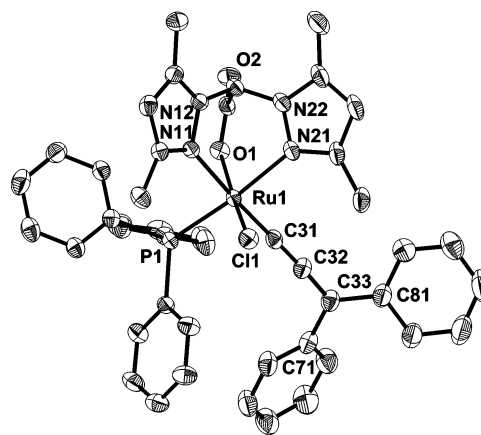


Figure 6. Molecular structure of $[\text{Ru}(\text{bdmpza})\text{Cl}(=\text{C}=\text{C}=\text{CPh}_2)(\text{PPh}_3)]$ (**5a-I**) with thermal ellipsoids drawn at the 50% probability level. Hydrogen atoms and solvent molecules are omitted for clarity.

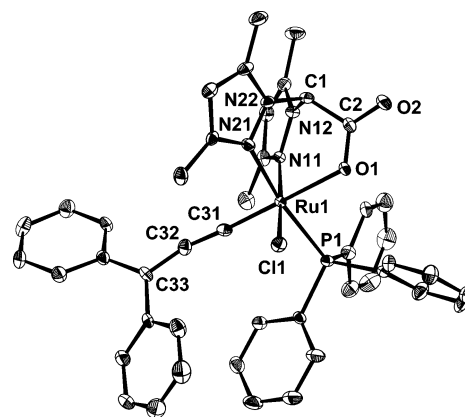


Figure 7. Molecular structure of $[\text{Ru}(\text{bdmpza})\text{Cl}(=\text{C}=\text{C}=\text{CPh}_2)(\text{PPh}_3)]$ (**5a-II**) with thermal ellipsoids drawn at the 50% probability level. Hydrogen atoms and solvent molecules are omitted for clarity.

Table 4. Selected Bond Lengths (Å) and Angles (deg) of the Allenylidene Complexes **5a-I** and **5a-II**

	5a-I	5a-II
Ru–N(11)	2.198(4)	2.096(4)
Ru–N(21)	2.189(4)	2.148(4)
Ru–O(1)	2.090(3)	2.151(3)
Ru–P	2.3348(16)	2.3603(18)
Ru–Cl	2.4158(17)	2.4228(18)
Ru–C(31)	1.886(5)	1.862(5)
C(31)–C(32)	1.266(7)	1.263(6)
C(32)–C(33)	1.362(7)	1.360(6)
N(11)–Ru–N(21)	83.87(15)	83.97(15)
O(1)–Ru–N(11)	84.24(14)	86.57(14)
O(1)–Ru–N(21)	85.54(15)	85.10(14)
O(1)–Ru–P	85.05(10)	85.88(10)
P–Ru–Cl	90.70(3)	88.64(6)
P–Ru–C(31)	88.14(15)	95.31(15)
O(1)–Ru–Cl	168.19(10)	91.33(10)
N(21)–Ru–P	170.55(12)	170.50(11)
N(11)–Ru–C(31)	175.22(17)	94.41(17)
Cl–Ru–C(31)	91.24(15)	87.52(14)
Ru–C(31)–C(32)	175.9(4)	175.0(4)
C(31)–C(32)–C(33)	176.3(6)	166.5(5)

the allenylidene complexes $[\text{Ru}(\text{bdmpza})(\text{Cl})(=\text{C}=\text{C}=\text{CPh}_2)(\text{PPh}_3)]$ (**5a-I/5a-II**) have been confirmed by two X-ray crystal structure analyses (Figures 6 and 7, Table 4). The configuration of **5a-I** around ruthenium corresponds to a slightly distorted octahedron and is analogous to those of the vinylidene complex **2b**, the carbonyl complex **3**, and the cyclic oxycarbene complex **4b**. The angles of the trans-arranged donors O(1)–Ru–Cl,

(49) Fürstner, A.; Guth, O.; Düffels, A.; Seidel, G.; Liebl, M.; Gabor, B. *Chem. Eur. J.* **2001**, *7*, 4811–4820.

(50) Schanz, H.-J.; Jafarpour, L.; Stevens, E. D.; Nolan, S. P. *Organometallics* **1999**, *18*, 5187–5190.

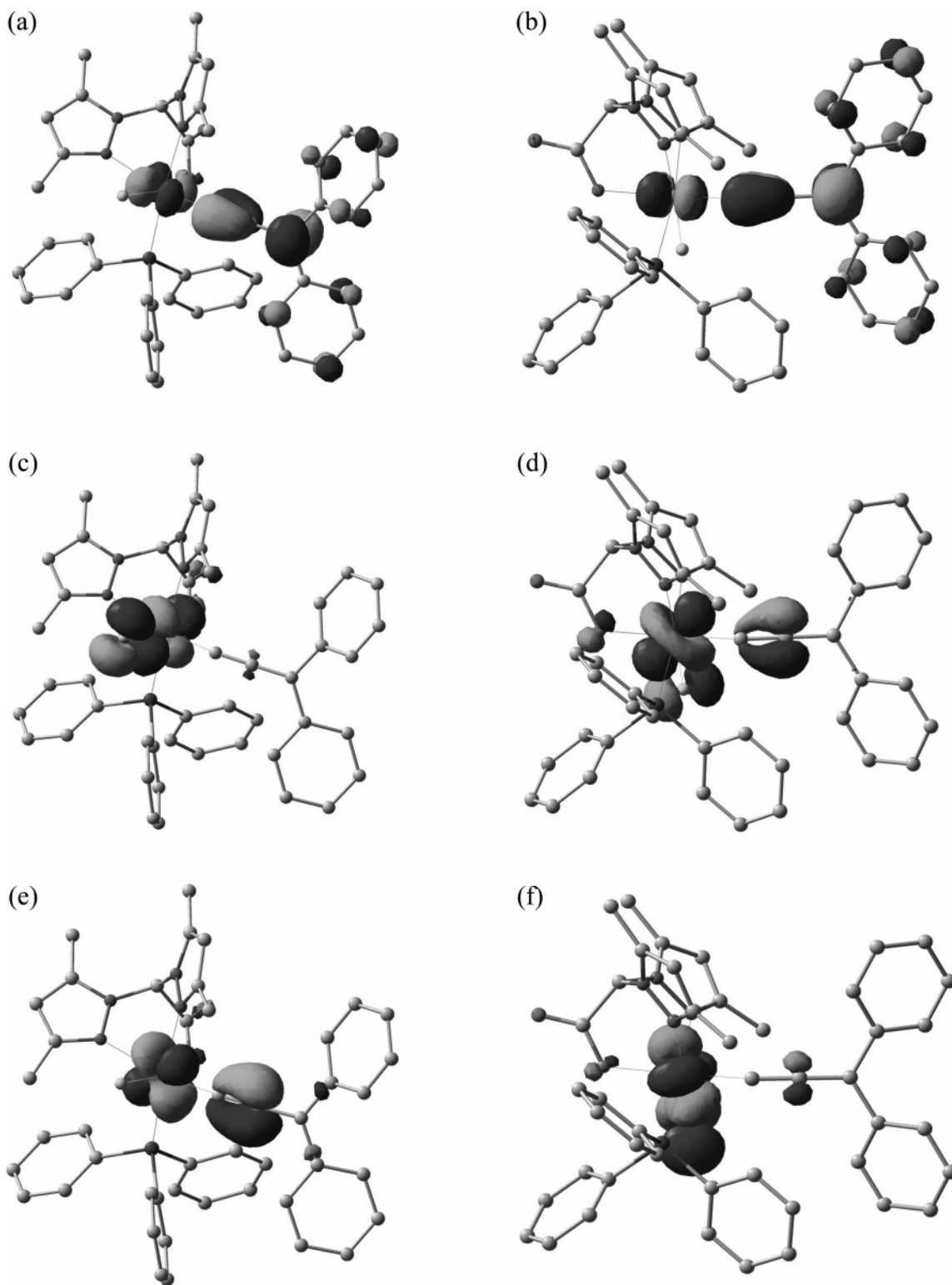


Figure 8. Contour plots of (a,b) the LUMO, (c,d) the HOMO, and (e,f) the HOMO-1 of $[\text{Ru}(\text{bdmpza})(\text{Cl})(=\text{C}=\text{C}=\text{CPh}_2)(\text{PPh}_3)]$ (**5a-I**/**5a-II**).

$\text{N}(21)\text{--Ru--P}(1)$, and $\text{N}(11)\text{--Ru--C}(31)$ are $168.19(10)$, $170.55(12)$, and $175.22(17)^\circ$, respectively. The distance $\text{Ru--C}(31)$ of **5a-I** ($1.886(5)$ Å) is almost the same as in the structurally related cationic and octahedral Tp allenylidene ruthenium complex $[\text{Ru}\{\kappa^3\text{-HB}(\text{pz})_3\}(\text{C}=\text{C}=\text{CPh}_2)(\text{PPh}_3)_2]\text{PF}_6$ ($1.889(3)$ Å) and somewhat longer than in neutral, penta-coordinated, 16-electron allenylidene ruthenium complexes such as $[\text{Ru}(\text{Cl})_2(\text{C}=\text{C}=\text{CPh}_2)(\text{PCy}_3)_2]$ ($1.794(11)$ Å).^{4,50} The allenylidene chain is close to linear ($\angle\text{Ru--C}(31)\text{--C}(32) =$

$175.9(4)^\circ$; $\angle\text{C}(31)\text{--C}(32)\text{--C}(33) = 176.3(6)^\circ$), with the phenyl residues slightly out of conjugation with the $\text{C}=\text{C}=\text{C}$ moiety.

The configuration of **5a-II** around ruthenium differs from the molecular structures of **5a-I**, **2b**, **3**, and **4b**. The allenylidene ligand in this type **B** structural isomer is arranged trans to the carboxylate donor of the bdpmpza ligand. Therefore, the $\text{Ru--C}(31)$ distance ($1.862(5)$ Å) and the $\text{Ru--N}(11)$ distance ($2.096(4)$ Å) are significantly shorter than those in the type **A** isomer **5a-I** (**5a-I**, $\text{Ru--N}(11) = 2.198(4)$ Å). This is due to a

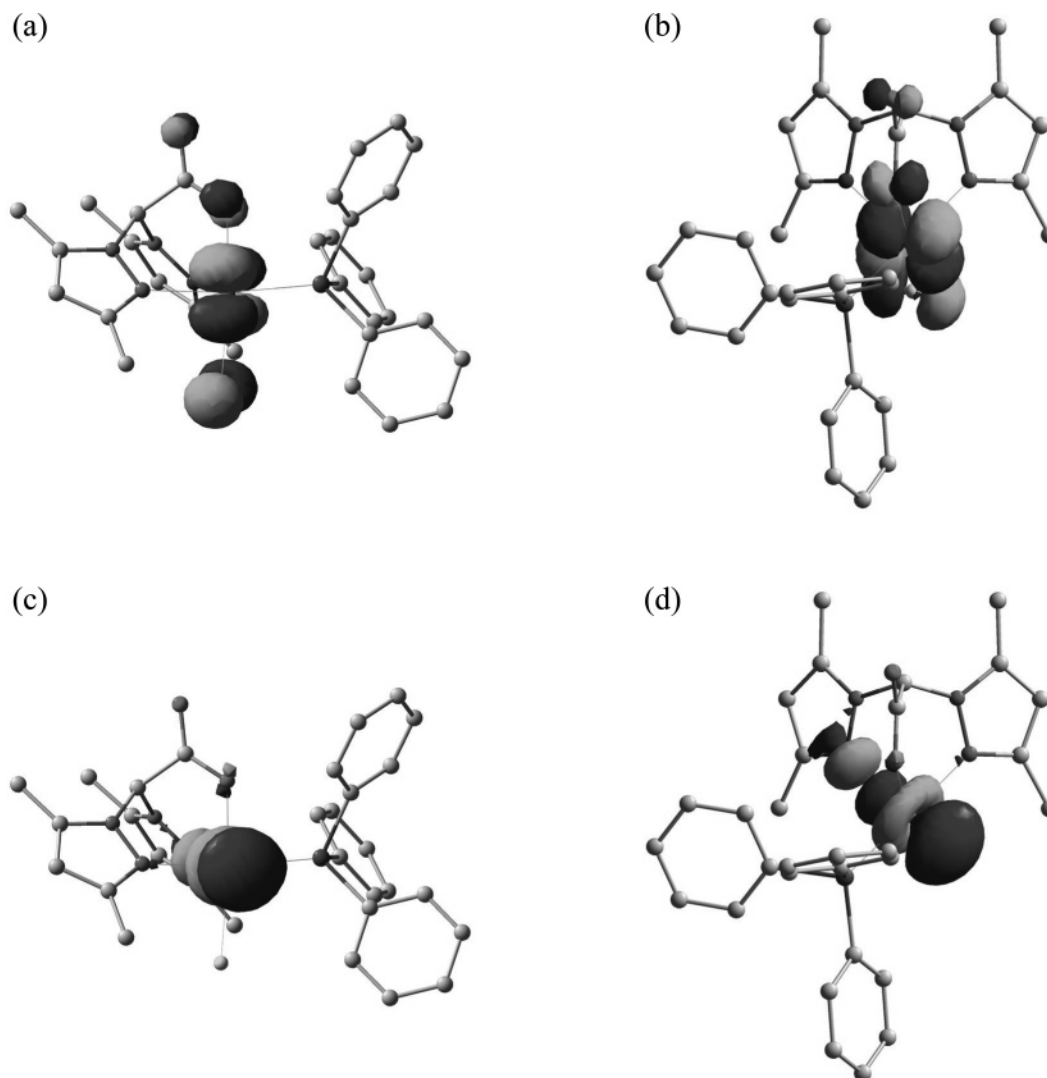


Figure 9. Contour plots of (a,b) the HOMO and (c,d) the LUMO of the 16-valence-electron fragment $[\text{Ru}(\text{bdmpza})\text{Cl}(\text{PPh}_3)]$.

trans influence in **5a-I** between the pyrazole and the allenylidene, which are both ligands with π -acceptor properties. The allenylidene chain is slightly kinked at the β -C ($\angle\text{Ru}-\text{C}(31)-\text{C}(32) = 175.0(4)^\circ$; $\angle\text{C}(31)-\text{C}(32)-\text{C}(33) = 166.3(5)^\circ$).

As mentioned above, both isomers of $[\text{Ru}(\text{bdmpza})\text{Cl}(\text{C}=\text{C}=\text{C}=\text{CPh}_2)(\text{PPh}_3)]$ (**5a-I/5a-II**) and $[\text{Ru}(\text{bdmpza})\text{Cl}(\text{C}=\text{C}=\text{C}=\text{CTol}_2)(\text{PPh}_3)]$ (**5b-I/5b-II**) show quite intense colors with the highest visible bands at $\lambda_{\text{max}} = 520$ (**5a-I**), 495 (**5a-II**), 533 (**5b-I**) and 507 nm (**5b-II**) (CH_2Cl_2). Similar intense colors in other ruthenium allenylidene complexes have been reported in the literature before and were assigned to metal to ligand charge transfer (MLCT) absorptions.^{51–53} To verify this hypothesis for **5a-I/5a-II** and **5b-I/5b-II**, DFT calculations were performed for both isomers of $[\text{Ru}(\text{bdmpza})\text{Cl}(\text{C}=\text{C}=\text{C}=\text{CPh}_2)(\text{PPh}_3)]$ (**5a-I/5a-II**), each calculation starting from the X-ray structure determination data. In both isomers the HOMO and HOMO-1 are mainly located at the metal center and the chloro ligand, while the LUMO is delocalized over the three double bonds and the aromatic rings (Figure 8).

This makes a MLCT quite reasonable. Nevertheless, none of our UV/vis data showed a significant change depending on solvent polarity: e.g., by using toluene instead of dichloromethane. Thus, due to this lack of a solvatochromic effect, this question remains unsolved so far. The calculations showed also a rather small energy difference between the type **A** and type **B** isomers. This agrees well with the experimental observations.

The resulting geometries of the DFT calculations were almost identical with the geometries of the X-ray structure determinations of $[\text{Ru}(\text{bdmpza})\text{Cl}(\text{C}=\text{C}=\text{C}=\text{CPh}_2)(\text{PPh}_3)]$ (**5a-I/5a-II**). Thus, these DFT calculations are also useful to study the orientation of the cumulenylidene ligands. Figure 9 shows contour plots of the HOMO and LUMO of the type **A** isomer 16-electron fragment $[\text{Ru}(\text{bdmpza})\text{Cl}(\text{PPh}_3)]$ from two different directions. It is obvious that especially the HOMO determines the orientation of the allenylidene ligand in $[\text{Ru}(\text{bdmpza})\text{Cl}(\text{C}=\text{C}=\text{C}=\text{CPh}_2)(\text{PPh}_3)]$ (**5a-I**). The ipso carbon atoms of the allenylidene phenyl groups are almost in a plane with N(11), N(21), P(1), C(31), and the ruthenium atom (Figure 6). This allows a perfect $\text{Ru}_{d\pi} \rightarrow \text{C}_{p\pi}$ back-donation of the fragment HOMO into the allenylidene π^* orbital, as depicted in Figure 10a.

Similar DFT calculations for the vinylidene complex $[\text{Ru}(\text{bdmpza})\text{Cl}(\text{C}=\text{C}=\text{CHTol})(\text{PPh}_3)]$ (**2b**) resulted in a geometry with the plane $\text{H}(32)-\text{C}(32)-\text{C}_{\text{ipso}}(\text{Tol})$ perpendicular

(51) Winter, R. F.; Klinkhammer, K.-W. *Organometallics* **2001**, *20*, 1317–1333.

(52) van Slageren, J.; Winter, R. F.; Klein, A.; Hartmann, S. *J. Organomet. Chem.* **2003**, *670*, 137–143.

(53) Mantovani, N.; Brugnati, M.; Gonsalvi, L.; Grigiotti, E.; Laschi, F.; Marvelli, L.; Peruzzini, M.; Reginato, G.; Rossi, R.; Zanello, P. *Organometallics* **2005**, *24*, 405–418.

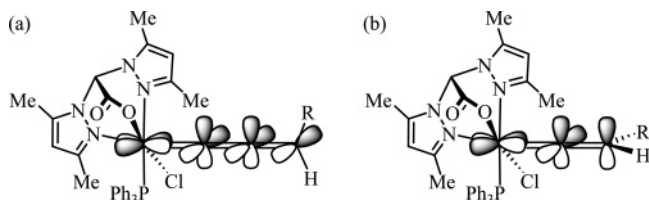


Figure 10. Coordination of (a) the allenylidene and (b) the vinylidene ligands by $\text{Ru}_{d\pi} \rightarrow \text{C}_{p\pi}$ back-donation.

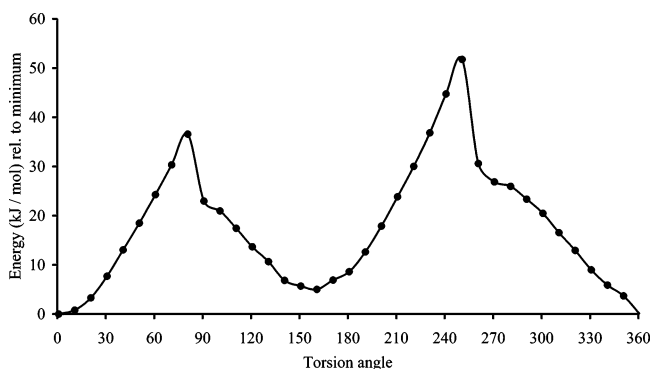


Figure 11. Rotational barrier of the vinylidene ligand in $[\text{Ru}(\text{bdmpza})(\text{Cl})(=\text{C}=\text{CHTol})(\text{PPh}_3)]$ (**2b**), calculated in 10° steps beginning from the structure of minimum energy.

to the plane $\text{N}(11)\text{--}\text{N}(21)\text{--}\text{P}(1)\text{--}\text{Ru}$. This is caused by $\text{Ru}_{d\pi} \rightarrow \text{C}_{p\pi}$ back-donation of the HOMO fragment into the vinylidene π^* orbital (Figure 10b). Surprisingly, the result of the structure determination of **2b** exhibits a slight deviation from this ideal perpendicular orientation by 20° . Therefore, the rotational barrier of the vinylidene ligand has been calculated in steps of 10° beginning from the structure of minimum energy (Figure 11).

A rotation of the vinylidene ligand by 20° causes a rather small increase in energy by 3 kJ/mol. Thus, the differences between the DFT geometry and the result of the X-ray structure determination might be due to crystal-packing effects. The effective maximum of the rotational barrier is found at 80° with an increase in energy of 37 kJ/mol. For the complex $[\text{Ru}\{\text{CH}_3\text{C}(\text{CH}_2\text{C}_5\text{H}_4)(\text{CH}_2\text{PPh}_2)_2\}\{\text{C}=\text{CHC}(\text{CH}_3)_3\}]\text{PF}_6$ the first indication for the coalescence was observed below 178 K.²⁸ Therefore, it is not really surprising that a dynamic ^1H NMR experiment at 183 K of complex **2b** did not show any signals other than those found at ambient temperature.

There have been numerous reports on the catalytic activity of ruthenium vinylidene and allenylidene complexes in olefin metathesis.^{6f,54,55} Therefore, the activity of **2a–d** and **5a,b** has been tested in ring-closing metathesis (RCM) of diethyl diallylmalonate, which is a convenient testing reaction frequently used to compare the activities of different ruthenium-based metathesis catalysts.⁵⁶ Disappointingly, irrespective of the reaction conditions used, no metathesis conversion was observed for any of the complexes tested. Addition of the phosphine scavenger CuCl ^{56,57} did not result in generation of the catalytic activity.

(54) (a) Katayama, H.; Ozawa, F. *Coord. Chem. Rev.* **2004**, *248*, 1703–1715. (b) Bruneau, C. Ruthenium Vinylidenes and Allenylidenes in Catalysis. In *Ruthenium Catalyst and Fine Chemistry*; Bruneau, C., Dixneuf, P. H., Eds.; Springer: Berlin, 2004.

(55) Castarlenas, R.; Fischmeister, C.; Bruneau, C.; Dixneuf, P. H. *J. Mol. Catal. A: Chem.* **2004**, *213*, 31–37.

(56) Dias, E. L.; Nguyen, S. T.; Grubbs, R. H. *J. Am. Chem. Soc.* **1997**, *119*, 3887–3897.

(57) Ulman, M.; Grubbs, R. H.; *J. Org. Chem.* **1999**, *64*, 7202–7207.

Concluding Remarks. Our results indicate that a rich chemistry is accessible from the complex $[\text{Ru}(\text{bdmpza})\text{Cl}(\text{PPh}_3)_2]$ (**1a**). Much of this has parallels with the chemistry of $[\text{Ru}(\eta^5\text{-C}_5\text{H}_5)\text{Cl}(\text{PPh}_3)_2]$ and especially $[\text{RuCl}\{\kappa^3\text{-HB}(\text{pz})_3\}(\text{PPh}_3)_2]$. Three advantages should, however, be noted in favor of the bdmpza versus the $\{\kappa^3\text{-HB}(\text{pz})_3\}$ or Cp chemistry. First, the conditions under which **1a** performs ligand exchange processes are a great deal milder than those of $[\text{Ru}(\eta^5\text{-C}_5\text{H}_5)\text{Cl}(\text{PPh}_3)_2]$ and even considerably milder compared to those of $[\text{RuCl}\{\kappa^3\text{-HB}(\text{pz})_3\}(\text{PPh}_3)_2]$. Second, the bdmpza ligand itself is quite robust and not affected by hydrolytic cleavage as, for example, the $\{\kappa^3\text{-HB}(\text{pz})_3\}$ ligand. Thus, many of the cumulenyldene complexes described here are extraordinarily resilient and can often be handled under aerobic and humid conditions for a short while. Third, the facially binding N,N,O ligand causes a differentiation of the remaining coordination sites regarding their π -basic nature. This allows the formation and separation of structural isomers with different chemical and physical properties. Finally, in future catalytic experiments the 18-electron ruthenium cumulenyldene complexes might be activated by protonation or alkylation of the bdmpza carboxylate donor and subsequent formation of 16-electron ruthenium cumulenyldene complexes. Future work in our laboratory will explore these effects. Efforts to prepare new ruthenium alkylidenes bearing the bdmpza ligand are also under way.

Experimental Section

All experiments were carried out with Schlenk techniques under an atmosphere of argon or N_2 . Solvents were dried by distillation over suitable drying agents (THF (Na), Et_2O (Na), pentane (LiAlH_4), hexane (Na), CH_2Cl_2 (CaH_2)) prior to use and were stored under N_2 . Flash chromatography was carried out on silica gel 60. IR: Biorad FTS 60, CaF_2 cuvettes (0.5 mm). ^1H NMR and ^{13}C NMR: Bruker AC 250, Bruker DRX 600 Avance, and Varian Unity Inova 400. ^{31}P NMR: JEOL GX 400, JEOL AL 400, and Varian Unity Inova 400. 2D NMR experiments: Bruker DRX 600 Avance and Varian Unity Inova 400. ^1H – ^{31}P -HMBC experiments: Bruker DRX 600 Avance and Varian Unity Inova 400. δ values are given relative to TMS (^1H), to solvent peaks (^{13}C), or to triphenylphosphine (-4.72 ppm) as internal standard (^{31}P). FAB MS: modified Finnigan MAT 312. GC: ThermoFinnigan TRACE GC/AS 2000. Elemental analyses: Analytical Laboratory of the Fachbereich Chemie, Universität Konstanz. A modified Siemens P4 diffractometer was used for X-ray structure determination.

Phenylacetylene, tolylacetylene, 1-hexyne, 1-pentyne, 3-butyn-1-ol, 4-pentyn-1-ol, ruthenium trichloride hydrate, and Grubbs' catalyst (first generation) were used as purchased. 1,1-Diphenyl-2-propyn-1-ol and 1,1-bis(4-methylphenyl)-2-propyn-1-ol were prepared according to the literature.⁵⁸ The syntheses of $[\text{Ru}(\text{bdmpza})\text{Cl}(\text{PPh}_3)_2]$ (**1a**) and $[\text{Ru}(\text{bpza})\text{Cl}(\text{PPh}_3)_2]$ (**1b**) were reported recently.²³ For differentiation of the NMR data the signals of the bdmpza ligand next to the PPh_3 ligand are marked with a prime.

Method A: General Procedure for the Syntheses of Vinylidene Complexes. To a suspension of $[\text{Ru}(\text{bdmpza})\text{Cl}(\text{PPh}_3)_2]$ in THF (50 mL) was added 1-alkyne, and the reaction mixture was stirred at ambient temperature. The progress of the reaction was monitored by IR spectroscopy. After the reaction was complete, the solvent was reduced in vacuo until precipitation occurred. Precipitation was completed by storing in a freezer (-30°C) for 20 h. The product was filtered off, washed with Et_2O (3×60 mL) and pentane (1×60 mL), and dried in vacuo.

(58) Brandsma, L. *Preparative Acetylenic Chemistry*, 2nd ed.; Elsevier: Amsterdam, 1988, p 92ff.

[Ru(bdmpza)Cl(PPh₃)₂](=C=CHPh) (2a). The reaction of [Ru(bdmpza)Cl(PPh₃)₂] (1.50 g, 1.65 mmol) in THF (50 mL) with phenylacetylene (0.910 mL, 8.25 mmol) for 4 h according to method A afforded two isomers of [Ru(bdmpza)Cl(PPh₃)₂](=C=CHPh) (2a) as a pink crystal powder.

Yield: 0.877 g (71%). Mp: 200 °C dec. IR (CH₂Cl₂): $\tilde{\nu}$ 1669 s (CO₂⁻), 1653 w, 1627 m, 1596 m, 1564 w (C=N), 1493 w, 1483 w, 1464 w, 1447 w, 1436 w cm⁻¹. FAB MS (NBOH matrix): *m/z* (relative intensity) 749 (31) [MH⁺], 713 (28) [M⁺ - Cl], 646 (100) [M⁺ - HC≡CPh], 611 (33) [M⁺ - Cl - HC≡CPh]. Anal. Calcd for C₃₈H₃₆ClN₄O₂PRu (748.23): C, 61.00; H, 4.85; N, 7.49. Found: C, 60.88; H, 5.00; N, 7.22. UV/vis (CH₂Cl₂): λ_{\max} (log ϵ) 233 (4.28), 290 nm (4.37). Major isomer: ¹H NMR (CDCl₃, 250 MHz) δ (ppm) 1.87 (s, 3H, Me³), 2.40 (s, 3H, Me³), 2.44 (s, 3H, Me⁵), 2.49 (s, 3H, Me⁵), 4.93 (d, 1H, ⁴J_{HP} = 4.9 Hz, H _{β}), 5.92 (s, 1H, H⁴), 5.94 (s, 1H, H⁴), 6.60 (s, 1H, CH), 6.71 (m, 2H, *m*-Ph), 6.89 (m, 1H, *p*-Ph), 7.01 (m, 2H, *o*-Ph), 7.21 (m, 6H, *m*-PPh₃), 7.31 (m, 3H, *p*-PPh₃), 7.55 (m, 6H, *o*-PPh₃); ¹³C NMR (CDCl₃, 62.9 MHz) δ (ppm) 11.0 (Me⁵), 11.2 (Me⁵), 14.2 (Me³), 14.4 (Me³), 68.4 (CH), 108.8 (C⁴), 108.9 (C⁴), 115.3 (d, ³J_{CP} = 4.4 Hz, C _{β}), 124.7 (*m*-Ph), 125.9 (*p*-Ph), 126.5 (*i*-Ph), 127.7 (d, ³J_{CP} = 10.9 Hz, *m*-PPh₃), 129.7 (*p*-PPh₃), 130.3 (*o*-Ph), 132.2 (d, ¹J_{CP} = 50.1 Hz, *i*-PPh₃), 134.1 (d, ²J_{CP} = 10.9 Hz, *o*-PPh₃), 139.9 (C⁵), 140.6 (C⁵), 155.1 (C³, C³), 166.7 (s, CO₂⁻), 362.5 (d, ²J_{CP} = 24.0 Hz, C _{α}); ³¹P NMR (CDCl₃, 161.8 MHz) δ (ppm) 37.5. Minor isomer (data extracted from spectra of a mixture with some signals partially covered by major isomer peaks): ¹H NMR (CDCl₃, 250 MHz) δ (ppm) 1.59 (s, 3H, Me³), 2.46 (s, 3H, Me³), 2.52 (s, 3H, Me⁵), 2.58 (s, 3H, Me⁵), 4.37 (d, 1H, ⁴J_{HP} = 4.0 Hz, H _{β}), 5.82 (s, H⁴, 1H), 6.60 (s, 1H, CH), 7.73 (m, 6H, *o*-PPh₃); ¹³C NMR (CDCl₃, 62.9 MHz) (signals partially covered by major isomer) δ (ppm) 11.8 (Me⁵), 15.1 (Me³), 15.2 (Me³), 68.5 (CH), 108.2 (C⁴), 113.1 (C _{β}), 127.8 (d, ³J_{CP} = 10.9 Hz, *m*-PPh₃), 129.5 (*p*-PPh₃), 130.1 (*o*-Ph), 132.6 (d, ¹J_{CP} = 48.0 Hz, *i*-PPh₃), 134.0 (d, ²J_{CP} = 10.9 Hz, *o*-PPh₃), 140.3 (C⁵), 141.3 (C⁵), 155.4 (C³, C³), 369.3 (d, ²J_{CP} = 24.0 Hz, C _{α}); ³¹P NMR (CDCl₃, 161.8 MHz) δ (ppm) 32.3.

[Ru(bdmpza)Cl(PPh₃)₂](=C=CHTol) (2b). Reaction of [Ru(bdmpza)Cl(PPh₃)₂] (1.50 g, 1.65 mmol) in THF (50 mL) with *p*-tolylacetylene (1.05 mL, 8.25 mmol) for 4 h according to method A afforded two isomers of [Ru(bdmpza)Cl(PPh₃)₂](=C=CHTol) (2b) as a pink crystalline powder.

Yield: 0.843 g (67%). Mp: 169 °C dec. IR (CH₂Cl₂): $\tilde{\nu}$ 1669 s (CO₂⁻), 1653 w, 1635 m, 1607 w, 1595 w, 1564 w (C=N), 1509 w, 1484 w, 1464 w, 1436 w cm⁻¹. FAB MS (NBOH matrix): *m/z* (relative intensity) 763 (17) [MH⁺], 727 (14) [M⁺ - Cl], 646 (100) [M⁺ - HC≡CTol-*p*], 611 (29) [M⁺ - Cl - HC≡C(Tol-*p*)]. Anal. Calcd for C₃₉H₃₈ClN₄O₂PRu (762.25): C, 61.45; H, 5.02; N, 7.35. Found: C, 61.30; H, 4.95; N, 7.07. UV/vis (CH₂Cl₂): λ_{\max} (log ϵ) 233 (4.57), 289 nm (4.39). Major isomer: ¹H NMR (CDCl₃, 250 MHz) δ (ppm) 1.89 (s, 3H, Me³), 2.28 (s, 3H, Me^{Tol}), 2.40 (s, 3H, Me³), 2.43 (s, 3H, Me⁵), 2.50 (s, 3H, Me⁵), 4.89 (d, 1H, ⁴J_{HP} = 4.9 Hz, H _{β}), 5.91 (s, 1H, H⁴), 5.94 (s, 1H, H⁴), 6.60 (s, 1H, CH), 6.63 (d, 2H, *J*_{HH} = 8.0 Hz, *o*-Tol), 6.87 (d, 2H, *J*_{HH} = 7.9 Hz, *m*-Tol), 7.22 (m, 6H, *m*-PPh₃), 7.32 (m, 3H, *p*-PPh₃), 7.73 (m, 6H, *o*-PPh₃); ¹³C NMR (CDCl₃, 62.9 MHz) δ (ppm) 11.0 (Me⁵), 11.2 (Me⁵), 14.2 (Me³), 14.3 (Me³), 21.1 (Me^{Tol}), 68.4 (CH), 108.8 (d, ⁴J_{CP} = 3.1 Hz, C⁴), 108.9 (C⁴), 115.1 (d, ³J_{CP} = 3.1 Hz, C _{β}), 126.6 (*o*-Tol), 127.7 (d, ³J_{CP} = 9.2 Hz, *m*-PPh₃), 128.7 (*m*-Tol), 129.7 (d, ⁴J_{CP} = 3.1 Hz, *p*-PPh₃), 130.1 (d, ⁴J_{CP} = 3.1 Hz, *i*-Tol), 132.4 (d, ¹J_{CP} = 48.8 Hz, *i*-PPh₃), 133.9 (*p*-Tol), 134.1 (d, ²J_{CP} = 9.2 Hz, *o*-PPh₃), 139.9 (C⁵), 140.6 (C⁵), 155.1 (C³, C³), 166.7 (CO₂⁻), 364.2 (d, ²J_{CP} = 24.4 Hz, C _{α}); ³¹P NMR (CDCl₃, 161.8 MHz) δ (ppm) 37.5. Minor isomer: ¹H NMR (CDCl₃, 250 MHz) (signals partially covered by major isomer) δ (ppm) 1.59 (s, 3H, Me³), 2.26 (s, 3H, Me^{Tol}), 2.45 (s, 3H, Me³), 2.46 (s, 3H, Me⁵), 2.51 (s, 3H, Me⁵), 4.27 (d, 1H, ⁴J_{HP} = 4.3 Hz, H _{β}), 5.79 (s, 1H, H⁴ or ⁴), 6.60 (s, 1H, CH), 6.47 (d, 2H, *J*_{HH} = 8.3 Hz, *o*-Tol), 6.80 (d, 2H, *J*_{HH}

= 8.2 Hz, *m*-Tol), 7.75 (m, 6H, *o*-PPh₃); ¹³C NMR (CDCl₃, 62.9 MHz) (only the signals of the PPh₃ ligand could be found) δ (ppm) 128.0 (d, ³J_{CP} = 9.2 Hz, *m*-PPh₃), 132.9 (d, ¹J_{CP} = 39.7 Hz, *i*-PPh₃); ³¹P NMR (CDCl₃, 161.8 MHz) δ (ppm) 32.6.

[Ru(bdmpza)Cl(PPh₃)₂](=C=CH(C₃H₇)) (2c). Reaction of [Ru(bdmpza)Cl(PPh₃)₂] (1.50 g, 1.65 mmol) in THF (50 mL) with 1-pentyne (0.813 mL, 8.25 mmol) for 4 h according to method A afforded [Ru(bdmpza)Cl(PPh₃)₂](=C=CH(C₃H₇)) (2c) as a pink crystalline powder.

Yield 0.625 g (53%). Mp: 152 °C dec. IR (CH₂Cl₂): ν 1667 s (CO₂⁻), 1653 sh, 1565 w (C=N), 1485 w, 1464 w, 1436 w, 1416 w cm⁻¹. FAB MS (NBOH matrix): *m/z* (relative intensity) 715 (19) [MH⁺], 679 (50) [M⁺ - Cl], 646 (100) [M⁺ - HC≡CPr], 611 (61) [M⁺ - Cl - HC≡CPr]. Anal. Calcd for C₃₅H₃₈ClN₄O₂PRu (714.21): C, 58.86; H, 5.36; N, 7.84. Found: C, 58.44; H, 5.34; N, 7.77. UV/vis (CH₂Cl₂): λ_{\max} (log ϵ) 234 nm (4.48). Major isomer: ¹H NMR (CD₂Cl₂, 400 MHz, multiplet signals for both isomers) δ (ppm) 0.74 (t, 3H, ³J_{HH} = 7.2 Hz, CH₃), 1.10 (m, 2H, 1 × CH₂), 1.51 (s, 3H, Me³), 2.02 (m, 2H, 1 × CH₂), 2.46 (s, 3H, Me³), 2.51 (s, 3H, Me⁵), 2.57 (s, 3H, Me⁵), 3.35 (doublet of triplets, 1H, ³J_{HH} = 7.6 Hz, ⁴J_{HP} = 3.9 Hz, H _{β}), 5.81 (s, 1H, H⁴), 6.00 (s, 1H, H⁴), 6.57 (s, H, CH), 7.31 (m, 9H, *m*-PPh₃, *p*-PPh₃), 7.70 (m, 6H, *o*-PPh₃); ¹³C NMR (CD₂Cl₂, 100.5 MHz) δ (ppm) 11.2, 11.9, 13.7, 14.5, 15.4, 21.0 (d, *J*_{CP} = 1.7 Hz), 24.7 (d, *J*_{CP} = 2.3 Hz) (CH₃, 2 × CH₂, Me³, Me³, Me⁵, Me⁵), 69.5 (CH), 106.9 (C⁴ or ⁴), 108.4 (C⁴ or ⁴), 108.5 (d, ³J_{CP} = 3.2 Hz, C _{β}), 128.0 (d, ³J_{CP} = 9.6 Hz, *m*-PPh₃), 129.9 (d, ⁴J_{CP} = 2.3 Hz, *p*-PPh₃), 133.9 (d, ¹J_{CP} = 46.1 Hz, *i*-PPh₃), 134.3 (d, ²J_{CP} = 9.2 Hz, *o*-PPh₃), 140.8 (d, ⁴J_{CP} = 1.6 Hz, C⁵), 143.1 (C⁵), 155.1 (d, ³J_{CP} = 2.2 Hz, C³), 155.4 (C³), 165.5 (CO₂⁻), 358.6 (d, ²J_{CP} = 17.5 Hz, C _{α}); ³¹P NMR (CDCl₃, 161.9 MHz) δ (ppm) 35.4. Minor isomer: ¹H NMR (CD₂Cl₂, 400 MHz, multiplet signals for both isomers) δ (ppm) 0.75 (t, 3H, ³J_{HH} = 7.2 Hz, CH₃), 1.10 (m, 2H, 1 × CH₂), 1.81 (s, 3H, Me³), 2.02 (m, 2H, 1 × CH₂), 2.46 (s, 3H, Me³), 2.50 (s, 3H, Me⁵), 2.59 (s, 3H, Me⁵), 3.85 (doublet of triplets, 1H, ³J_{HH} = 7.8 Hz, ⁴J_{HP} = 4.6 Hz, H _{β}), 5.95 (s, 1H, H⁴), 6.01 (s, 1H, H⁴), 6.54 (s, H, CH), 7.31 (m, 9H, *m*-PPh₃, *p*-PPh₃), 7.70 (m, 6H, *o*-PPh₃); ¹³C NMR (CD₂Cl₂, 100.5 MHz) δ (ppm) 11.2, 11.4, 13.7, 14.3, 14.8, 20.6 (d, *J*_{CP} = 2.0 Hz), 24.7 (d, *J*_{CP} = 2.3 Hz), (CH₃, 2 × CH₂, Me³, Me³, Me⁵, Me⁵), 69.0 (CH), 106.9 (C⁴ or ⁴), 108.4 (C⁴ or ⁴), 108.1 (d, ³J_{CP} = 3.4 Hz, C _{β}), 127.9 (d, ³J_{CP} = 9.6 Hz, *m*-PPh₃), 130.0 (d, ⁴J_{CP} = 2.4 Hz, *p*-PPh₃), 133.4 (d, ¹J_{CP} = 47.4 Hz, *i*-PPh₃), 134.3 (d, ²J_{CP} = 9.2 Hz, *o*-PPh₃), 140.7 (d, ⁴J_{CP} = 1.8 Hz, C⁵), 141.4 (C⁵), 155.3 (d, ³J_{CP} = 2.0 Hz, C³), 155.3 (C³), 166.5 (CO₂⁻), 355.9 (d, ²J_{CP} = 24.5 Hz, C _{α}); ³¹P NMR (CDCl₃, 161.9 MHz) δ (ppm) 40.8.

[Ru(bdmpza)Cl(PPh₃)₂](=C=CH(C₄H₉)) (2d). Reaction of [Ru(bdmpza)Cl(PPh₃)₂] (1.50 g, 1.65 mmol) in THF (50 mL) with 1-hexyne (0.953 mL, 8.25 mmol) for 4 h according to method A afforded [Ru(bdmpza)Cl(PPh₃)₂](=C=CH(C₄H₉)) (2d) as a pink crystalline powder.

Yield 0.745 g (62%). Mp: 140 °C dec. IR (CH₂Cl₂): $\tilde{\nu}$ 1669 s (CO₂⁻), 1653 sh, 1565 w (C=N), 1484 w, 1464 w, 1436 w cm⁻¹. FAB MS (NBOH matrix): *m/z* (relative intensity) 729 (19) [MH⁺], 693 (24) [M⁺ - Cl], 646 (100) [M⁺ - HC≡CBu], 611 (51) [M⁺ - Cl - HC≡CBu]. Anal. Calcd for C₃₆H₄₀ClN₄O₂PRu (728.24): C, 59.38; H, 5.54; N, 7.69. Found: C, 59.34; H, 5.81; N, 7.33. UV/vis (CH₂Cl₂): λ_{\max} (log ϵ) 234 nm (4.44). ¹H NMR (CDCl₃, 250 MHz): δ (ppm) 0.77 (t, together 6H, ³J_{HH} = 7.2 Hz, 2 × CH₃), 1.07, 2.07 (m, together 12H, 6 × CH₂), 1.54, 1.85 (s, together 6H, 2 × Me³), 2.43, 2.45 (s, together 6H, 2 × Me³), 2.48, 2.49 (s, together 6H, 2 × Me⁵), 2.59, 2.62 (s, together 6H, 2 × Me⁵), 3.30 (doublet of triplets, 1H, ³J_{HH} = 7.6 Hz, ⁴J_{HP} = 4.0 Hz, H _{β}), 3.85 (doublet of triplets, 1H, ³J_{HH} = 7.8 Hz, ⁴J_{HP} = 4.6 Hz, H _{β}), 5.78, 5.91 (s, together 2H, 2 × H⁴), 5.96 (s, 2H, 2 × H⁴), 6.56, 6.60 (s, together 2H, 2 × CH), 7.30 (m, together 18H, 2 × *m*-PPh₃, 2 × *p*-PPh₃), 7.51, 7.75 (m, together 12H, 2 × *o*-PPh₃).

^{13}C NMR (acetone- d_6 , 62.9 MHz): δ (ppm) 10.9, 11.0, 11.1, 11.5, 14.0, 14.1, 14.5, 14.6, 14.8, 15.7, 18.4, 18.6, 22.8, 22.8, 34.0, 34.1 ($2 \times \text{CH}_3$, $6 \times \text{CH}_2$, $2 \times \text{Me}^3$, $2 \times \text{Me}^3$, $2 \times \text{Me}^5$, $2 \times \text{Me}^5$), 69.5, 70.0 ($2 \times \text{CH}$), 106.7 (C^4 or $4'$), 108.5 (d, $J_{\text{CP}} = 4.3$ Hz, C_β), 108.7 (C^4 or $4'$), 108.8 (d, $J_{\text{CP}} = 4.3$ Hz, C_β), 109.0, 109.1 ($2 \times \text{C}^4$ or $4'$), 128.2 (*m*-PPh $_3$), 130.3 (*p*-PPh $_3$), 134.2 (d, $^1J_{\text{CP}} = 47.7$ Hz, *i*-PPh $_3$), 135.0 (*o*-PPh $_3$), 135.0 (d, $^1J_{\text{CP}} = 45.5$ Hz, *i*-PPh $_3$), 141.7, 142.4, 144.5 ($2 \times \text{C}^5$, $2 \times \text{C}^5$), 155.0, 155.3, 155.4, 155.5 ($2 \times \text{C}^3$, $2 \times \text{C}^3$), 165.5, 166.2 ($2 \times \text{CO}_2^-$), 355.0 (d, $J_{\text{CP}} = 26.2$ Hz, C_α), 359.2 (d, $J_{\text{CP}} = 17.4$ Hz, C_α). ^{31}P NMR (CDCl $_3$, 161.8 MHz): δ (ppm) 40.6, 35.4.

Formation of [Ru(bdmpza)Cl(CO)(PPh $_3$)] (3). A solution of [Ru(bdmpza)Cl(PPh $_3$) $_2$] (**1a**) (1.50 g, 1.650 mmol) in THF (20 mL) and CH $_2$ Cl $_2$ (30 mL) was flushed for 8 h with a slight stream of CO gas. Reducing of the solvent in vacuo to 3–5 mL and precipitating the product with *n*-hexane afforded [Ru(bdmpza)Cl(PPh $_3$)(CO)] (**3**) as a yellow crystalline powder. Identical samples of **3** were also obtained by exposing solutions of the ruthenium vinylidene complexes [Ru(bdmpza)Cl(=C=CHR)(PPh $_3$)] (**2a–d**) in THF to air.

Yield: 901 mg (81%). Mp: 174 °C dec. IR (CH $_2$ Cl $_2$): $\tilde{\nu}$ 1969 s (CO), 1667 s (CO $_2^-$), 1646 sh, 1565 w (C=N), 1484 w, 1464 w, 1450 w, 1436 w, 1417 w cm $^{-1}$. FAB MS (NBOH matrix): *m/z* (relative intensity) 674 (31) [M $^+$], 646 (33) [M $^+$ – CO], 639 (100) [M $^+$ – Cl]. Anal. Calcd for C $_{31}$ H $_{30}$ ClN $_4$ O $_3$ PRu (674.10): C, 55.24; H, 4.49; N, 8.31. Found: C, 55.42; H, 4.79; N, 8.18. UV/vis (CH $_2$ Cl $_2$): λ_{max} (log ϵ) 267 nm (3.81). ^1H NMR (CDCl $_3$, 600 MHz): δ (ppm) 1.91 (s, 3H, Me 3), 2.42 (s, 3H, Me 5), 2.47 (s, 3H, Me 5), 2.68 (s, 3H, Me 3), 5.90 (s, 1H, H 4), 6.00 (s, 1H, H 4), 6.52 (s, 1H, CH), 7.31 (m, 6H, *m*-PPh $_3$), 7.38 (m, 3H, *p*-PPh $_3$), 7.51 (m, 6H, *o*-PPh $_3$). ^{13}C NMR (CD $_2$ Cl $_2$, 150 MHz): δ (ppm) 11.0 (Me 5), 11.2 (Me 5), 14.4 (Me 3), 14.6 (Me 3), 68.6 (CH), 108.9 (C 4), 109.0 (C 4), 127.9 (d, $^3J_{\text{CP}} = 9.6$ Hz, *m*-PPh $_3$), 130.1 (*p*-PPh $_3$), 132.2 (d, $^1J_{\text{CP}} = 47.6$ Hz, *i*-PPh $_3$), 134.0 (d, $^2J_{\text{CP}} = 9.5$ Hz, *o*-PPh $_3$), 140.6 (C 5), 141.3 (C 5), 155.6 (C 3), 156.2 (C 3), 166.1 (CO $_2^-$), 202.6 (d, $^2J_{\text{CP}} = 19.8$ Hz, C_α). ^{31}P NMR (CDCl $_3$, 161.9 MHz): δ (ppm) 41.7.

Method B: General Procedure for the Syntheses of Cyclic Carbene Complexes. To a suspension of [Ru(bdmpza)Cl(PPh $_3$) $_2$] in THF (50 mL) was added the terminal alkynol, and the reaction mixture was stirred at ambient temperature. The progress of the reaction was monitored by IR spectroscopy. After the reaction was complete, the solvent was reduced in vacuo. The precipitate was washed with pentane (5×60 mL) and dried in vacuo.

[Ru(bdmpza)Cl(=C(CH $_2$) $_3$ O)(PPh $_3$)] (4a). Reaction of [Ru(bdmpza)Cl(PPh $_3$) $_2$] (1.50 g, 1.65 mmol) with 3-butyn-1-ol (190 μL , 2.51 mmol) for 72 h according to method B afforded two isomers of the complex [Ru(bdmpza)Cl(=C(CH $_2$) $_3$ O)(PPh $_3$)] (**4a**) as a yellow crystalline powder.

Yield: 0.936 g (79%). Mp: 208 °C. IR (CH $_2$ Cl $_2$): $\tilde{\nu}$ 1660 s (CO $_2^-$), 1564 w (C=N), 1483 w, 1463 w, 1435 w, 1419 w. FAB MS (NBOH matrix): *m/z* (relative intensity) 716 (100) [M $^+$], 681 (41) [M $^+$ – Cl]. Anal. Calcd for C $_{34}$ H $_{36}$ ClN $_4$ O $_3$ PRu (716.17): C, 57.02; H, 5.07; N, 7.82. Found: C, 56.74; H, 5.16; N, 7.42. UV/vis (CH $_2$ Cl $_2$): λ_{max} (log ϵ) 235 (4.41), 305 nm (3.86). **4a-I** (carbene trans to pyrazole): ^1H NMR (CD $_2$ Cl $_2$, 600 MHz) δ (ppm) 1.63 (m, 1H, ring-H 4) 1.73 (m, 1H, ring-H 4), 2.04 (s, 3H, Me 3), 2.12 (s, 3H, Me 3), 2.51 (s, 3H, Me 5), 2.57 (s, 3H, Me 5), 2.71 (m, 1H, ring-H 5), 2.98 (m, 1H, ring-H 5), 3.86 (m, 1H, ring-H 3), 4.66 (m, 1H, ring-H 3), 6.01 (s, 1H, H 4), 6.03 (s, 1H, H 4), 6.64 (s, 1H, CH), 7.26 (m, 6H, *m*-PPh $_3$), 7.32 (m, 3H, *p*-PPh $_3$), 7.70 (m, 6H, *o*-PPh $_3$); ^{13}C NMR (CD $_2$ Cl $_2$, 150 MHz) δ (ppm) 11.4 (Me 3 , Me 5), 14.2 (Me 3), 14.8 (Me 3), 22.2 (ring-C 4), 52.3 (ring-C 5), 69.6 (CH), 81.1 (ring-C 3), 108.6 (C 4), 108.8 (C 4), 127.7 (d, $^2J_{\text{CP}} = 9.1$ Hz, *m*-PPh $_3$), 129.5 (*p*-PPh $_3$), 134.3 (d, $^3J_{\text{CP}} = 8.9$ Hz, *o*-PPh $_3$), 135.2 (d, $^1J_{\text{CP}} = 42.0$ Hz, *i*-PPh $_3$), 141.0 (C 5), 141.9 (C 5), 153.9 (C 3), 156.5 (C 3), 167.2

(CO $_2^-$), 311.9 (d, $^2J_{\text{CP}} = 16.6$ Hz, C_α); ^{31}P NMR (CDCl $_3$, 161.9 MHz) δ (ppm) 44.5. **4a-II** (carbene trans to carboxylate): ^1H NMR (CD $_2$ Cl $_2$, 600 MHz) δ (ppm) 1.27 (s, 3H, Me 3), 1.47 (m, 1H, ring-H 5) 1.55 (m, 1H, ring-H 4), 1.76 (m, 1H, ring-H 4), 2.05 (s, 3H, Me 3), 2.48 (s, 3H, Me 5), 2.51 (s, 3H, Me 5), 2.75 (m, 1H, ring-H 5), 4.31 (m, 1H, ring-H 3), 4.41 (m, 1H, ring-H 3), 5.72 (s, 1H, H 4), 5.97 (s, 1H, H 4), 6.59 (s, 1H, CH), 7.26 (m, 6H, *m*-PPh $_3$), 7.32 (m, 3H, *p*-PPh $_3$), 7.70 (m, 6H, *o*-PPh $_3$); ^{13}C NMR (CD $_2$ Cl $_2$, 150 MHz) δ (ppm) 11.3 (Me 5), 11.8 (Me 5), 14.1 (Me 3), 15.5 (Me 3), 23.5 (ring-C 4), 51.3 (ring-C 5), 69.7 (CH), 79.5 (ring-C 3), 108.1 (C 4), 108.5 (C 4), 127.9 (d, $^2J_{\text{CP}} = 9.1$ Hz, *m*-PPh $_3$), 129.4 (*p*-PPh $_3$), 134.7 (d, $^3J_{\text{CP}} = 8.4$ Hz, *o*-PPh $_3$), 135.7 (d, $^1J_{\text{CP}} = 44.8$ Hz, *i*-PPh $_3$), 140.8 (C 5), 142.0 (C 5), 153.9 (C 3), 154.5 (C 3), 166.4 (CO $_2^-$), 311.1 (d, $^2J_{\text{CP}} = 14.3$ Hz, C_α); ^{31}P NMR (CDCl $_3$, 161.9 MHz) δ (ppm) 38.3.

[Ru(bdmpza)Cl(=C(CH $_2$) $_4$ O)(PPh $_3$)] (4b). Reaction of [Ru(bdmpza)Cl(PPh $_3$) $_2$] (1.50 g, 1.65 mmol) with 4-pentyn-1-ol (230 μL , 2.51 mmol) for 72 h according to method B afforded two isomers of the complex [Ru(bdmpza)Cl(=C(CH $_2$) $_4$ O)(PPh $_3$)] (**4b**) as a yellow crystalline powder.

Yield: 0.976 g (81%). Mp: 177 °C dec. IR (CH $_2$ Cl $_2$): $\tilde{\nu}$ 1663 s (CO $_2^-$), 1607 w, 1565 w (C=N), 1483 w, 1463 w, 1435 w, 1419 w. FAB MS (NBOH matrix): *m/z* (relative intensity) 730 (100) [M $^+$], 695 (68) [M $^+$ – Cl], 646 (31) [M $^+$ – C $_5$ H $_7$ O], 611 (24) [M $^+$ – Cl – C $_5$ H $_7$ O]. Anal. Calcd for C $_{35}$ H $_{38}$ ClN $_4$ O $_3$ PRu (730.20): C, 57.57; H, 5.25; N, 7.67. Found: C, 57.81; H, 5.27; N, 7.25. UV/vis (CH $_2$ Cl $_2$): λ_{max} (log ϵ) 244 (4.20), 313 nm (3.85). **4b-I** (carbene trans to pyrazole): ^1H NMR (CD $_2$ Cl $_2$, 400 MHz) δ (ppm) 1.43 (m, 3H, $2 \times$ ring-H 5 , $1 \times$ ring-H 4), 1.73 (m, 1H, ring-H 4), 2.02 (s, 3H, Me 3), 2.72 (m, 1H, ring-H 6), 2.93 (m, 1H, ring-H 6), 2.25 (s, 3H, Me 3), 2.51 (s, 3H, Me 5), 2.56 (s, 3H, Me 5), 3.70 (m, 1H, ring-H 3), 4.48 (m, 1H, ring-H 5), 5.99 (s, 1H, H 4), 6.03 (s, 1H, H 4), 6.64 (s, 1H, CH), 7.26 (m, 6H, *m*-PPh $_3$), 7.31 (m, 3H, *p*-PPh $_3$), 7.33 (m, 6H, *o*-PPh $_3$); ^{13}C NMR (CD $_2$ Cl $_2$, 100.5 MHz) δ (ppm) 11.4 (Me 5), 11.5 (Me 5), 14.6 (Me 3), 14.8 (Me 3), 18.1 (ring-C 5), 22.2 (ring-C 4), 46.5 (ring-C 6), 69.7 (CH), 73.7 (ring-C 3), 108.7 (d, $^4J_{\text{CP}} = 2.6$ Hz, C 4), 108.8 (C 4), 127.7 (d, $^2J_{\text{CP}} = 9.2$ Hz, *m*-PPh $_3$), 129.3 (*p*-PPh $_3$), 134.4 (d, $^3J_{\text{CP}} = 9.0$ Hz, *o*-PPh $_3$), 136.0 (d, $^1J_{\text{CP}} = 43.5$ Hz, *i*-PPh $_3$), 140.9 (C 5), 141.7 (C 5), 153.9 (C 3), 156.4 (C 3), 167.3 (CO $_2^-$), 315.7 (d, $^2J_{\text{CP}} = 16.1$ Hz, C_α). ^{31}P NMR (CDCl $_3$, 161.9 MHz): δ (ppm) 45.6. **4b-II** (carbene trans to carboxylate): ^1H NMR (CD $_2$ Cl $_2$, 600 MHz) δ (ppm) 1.24 (m, 1H, ring-H 5), 1.34 (m, 1H, ring-H 5), 1.35 (s, 3H, Me 3), 1.64 (m, 2H, ring-H 4), 2.02 (m, 1H, ring-H 6), 2.20 (s, 3H, Me 3), 2.50 (s, 3H, Me 5), 2.52 (s, 3H, Me 5), 2.69 (m, 1H, ring-H 6), 4.09 (m, 2H, ring-H 5), 5.73 (s, 1H, H 4), 5.99 (s, 1H, H 4), 6.61 (s, 1H, CH), 7.24 (m, 6H, *m*-PPh $_3$), 7.30 (m, 3H, *p*-PPh $_3$), 7.71 (m, 6H, *o*-PPh $_3$); ^{13}C NMR (CD $_2$ Cl $_2$, 150 MHz) δ (ppm) 11.1 (Me 5), 11.5 (Me 5), 14.3 (Me 3), 15.6 (Me 3), 17.3 (ring-C 5), 21.9 (ring-C 4), 46.9 (ring-C 6), 69.3 (CH), 72.1 (ring-C 3), 108.1 (C 4), 108.6 (C 4), 127.7 (d, $^2J_{\text{CP}} = 9.0$ Hz, *m*-PPh $_3$), 129.3 (*p*-PPh $_3$), 134.7 (d, $^3J_{\text{CP}} = 8.0$ Hz, *o*-PPh $_3$), 135.5 (d, $^1J_{\text{CP}} = 41.0$ Hz, *i*-PPh $_3$), 140.7 (C 5), 141.8 (C 5), 153.8 (C 3), 154.0 (C 3), 166.5 (CO $_2^-$), 314.5 (C_α); ^{31}P NMR (CDCl $_3$, 161.9 MHz) δ (ppm) 38.7.

Method C: General Procedure for the Syntheses of Allenylidene Complexes. To a suspension of [Ru(bdmpza)Cl(PPh $_3$) $_2$] (**1a**) in THF (50 mL) was added the 1,1-diaryl-2-propyne-1-ol, and the reaction mixture was stirred for 48 h at ambient temperature and finally heated under reflux for 4 h. The progress of the reaction was monitored by IR spectroscopy. The solvent was evaporated in vacuo and loaded with a small portion of CH $_2$ Cl $_2$ on a column of silica (length 15 cm, i.d. 4 cm). The column was washed with pentane and Et $_2$ O, and the product was eluted using CH $_2$ Cl $_2$ /acetone (1:1 v/v). Separation of the isomers was achieved by an additional column chromatography step (CH $_2$ Cl $_2$ /acetone, 1:1 v/v) on a longer column (silica gel, length 40 cm, i.d. 4 cm). The fractions were evaporated in vacuo and precipitated from CH $_2$ Cl $_2$ (1 mL) with pentane. The products were filtered off and dried in vacuo.

[Ru(bdmpza)Cl(PPh₃)(\equiv C=C=CPh₂)] (5a-I/5a-II). Reaction of [Ru(bdmpza)Cl(PPh₃)₂] (1.50 g, 1.65 mmol) in THF (50 mL) with 1,1-diphenyl-2-propyn-1-ol (0.515 g, 2.48 mmol) according to method C yielded two isomers of [(bdmpza)Cl(PPh₃)Ru(\equiv C=C=CPh₂)] (**5a-I/5a-II**) as a purple crystalline powder.

Yield 0.787 g (57%). Anal. Calcd for C₄₅H₄₀ClN₄O₂PRu (836.33): C, 64.63; H, 4.82; N, 6.70. Found: C, 64.25; H, 5.19; N, 6.48. Violet isomer **5a-I**: mp 153 °C dec; IR (CH₂Cl₂) $\tilde{\nu}$ 1918 w (C=C=C), 1663 s (CO₂⁻), 1653 sh, 1565 w (C=N), 1484 w, 1464 w, 1436 w cm⁻¹; FAB MS (NBOH matrix) *m/z* (relative intensity) 836 (100) [M⁺], 801 (33) [M⁺ - Cl], 646 (11) [M⁺ - C₃Ph₂]; UV/vis (CH₂Cl₂) λ_{\max} (log ϵ) 233 (4.52), 338 (3.97), 520 nm (4.21); UV/vis (toluene) λ_{\max} (log ϵ) 283 (4.20), 344 (3.95), 519 nm (4.22); ¹H NMR (CDCl₃, 600 MHz) δ (ppm) 1.92 (s, 3H, Me³), 2.19 (s, 3H, Me³), 2.47 (s, 3H, Me⁵), 2.55 (s, 3H, Me⁵), 5.87 (s, 1H, H⁴), 6.01 (s, 1H, H⁴), 6.64 (s, 1H, CH), 7.13 (m, 4H, *m*-Ph), 7.16 (m, 6H, *m*-PPh₃), 7.28 (m, 3H, *p*-PPh₃), 7.48 (m, 6H, *o*-PPh₃), 7.54 (m, 2H, *p*-Ph), 7.57 (m, 4H, *o*-Ph); ¹³C NMR (CDCl₃, 150.9 MHz) δ (ppm) 11.0 (Me⁵), 11.3 (Me⁵), 13.5 (Me³), 14.4 (Me³), 68.8 (CH), 108.2 (C⁴), 109.1 (C⁴), 127.5 (d, ²J_{CP} = 9.7 Hz, *m*-PPh₃), 128.7 (*p*-Ph, *m*-Ph), 129.0 (*o*-Ph), 129.5 (*p*-PPh₃), 133.3 (d, ¹J_{CP} = 46.5 Hz, *i*-PPh₃), 134.2 (d, ²J_{CP} = 9.2 Hz, *o*-PPh₃), 139.3 (C⁵), 140.7 (C⁵), 142.1 (C _{γ}), 146.1 (*i*-Ph), 154.9 (C³), 155.8 (C³), 166.6 (CO₂⁻), 227.4 (C _{β}), 305.5 (d, ²J_{CP} = 26.4 Hz, C _{α}); ³¹P NMR (CDCl₃, 161.8 MHz) δ (ppm) 37.3. Red isomer **5a-II**: mp 219 °C dec; IR (CH₂Cl₂) $\tilde{\nu}$ 1918 w (C=C=C), 1666 s (CO₂⁻), 1565 w (C=N), 1484 w, 1464 w, 1436 w cm⁻¹; FAB MS (NBOH matrix) *m/z* (relative intensity) 836 (87) [M⁺], 801 (100) [M⁺ - Cl], 646 (26) [M⁺ - C₃Ph₂]; UV/vis (CH₂Cl₂) λ_{\max} (log ϵ) 232 (4.53), 339 (3.94), 495 nm (4.24); UV/vis (toluene) λ_{\max} (log ϵ) 281 (4.23), 498 nm (4.22); ¹H NMR (CD₂Cl₂, 600 MHz) δ (ppm) 1.36 (s, 3H, Me³), 2.15 (s, 3H, Me³), 2.48 (s, 3H, Me⁵), 2.53 (s, 3H, Me⁵), 5.74 (s, 1H, H⁴), 5.87 (s, 1H, H⁴), 6.68 (s, 1H, CH), 7.12 (m, 6H, *m*-PPh₃), 7.23 (m, 7H, *m*-Ph, *p*-PPh₃), 7.57 (vt, 6H, *o*-PPh₃), 7.62 (vt, 2H, *p*-Ph), 7.69 (vd, 4H, *o*-Ph); ¹³C NMR (CD₂Cl₂, 62.9 MHz) δ (ppm) 11.1 (Me⁵), 11.8 (Me⁵), 13.7 (Me³), 14.4 (Me³), 69.7 (CH), 108.2 (C⁴), 108.6 (C⁴), 127.8 (d, ²J_{CP} = 9.7 Hz, *m*-PPh₃), 129.2 (*m*-Ph), 129.4 (*o*-Ph), 129.6 (*p*-Ph), 129.9 (*p*-PPh₃), 133.5 (d, ¹J_{CP} = 46.5 Hz, *i*-PPh₃), 134.6 (d, ²J_{CP} = 9.3 Hz, *o*-PPh₃), 140.5 (C⁵), 142.5 (C⁵), 147.0 (*i*-Ph), 149.2 (C _{γ}), 154.7 (C³), 156.0 (C³), 166.0 (CO₂⁻), 239.7 (C _{β}), 314.7 (d, ²J_{CP} = 19.1 Hz, C _{α}); ³¹P NMR (CDCl₃, 161.8 MHz) δ (ppm) 32.3.

[Ru(bdmpza)Cl(PPh₃)(\equiv C=C=CTol₂)] (5b-I/5b-II). Reaction of [(bdmpza)Cl(PPh₃)₂Ru] (1.50 g, 1.65 mmol) in THF (50 mL) with 1,1-bis(4-methylphenyl)-2-propyn-1-ol (0.780 g, 3.30 mmol) according to method C yielded two isomers of [(bdmpza)Cl(PPh₃)Ru(\equiv C=C=CTol₂)] (**5b-I/5b-II**) as a purple crystal powder.

Yield 0.670 g (47%). Anal. Calcd for C₄₇H₄₄ClN₄O₂PRu (864.39): C, 65.31; H, 5.13; N, 6.48. Found: C, 65.64; H, 5.24; N, 6.12. Violet isomer **5b-I**: mp 211 °C dec; IR (CH₂Cl₂) $\tilde{\nu}$ 1919 w (C=C=C), 1663 s (CO₂⁻), 1644 sh, 1603 w, 1564 w (C=N), 1483 w, 1463 w, 1436 w cm⁻¹; MS FAB (NBOH matrix) *m/z* (relative intensity) 864 (100) [M⁺], 829 (81) [M⁺ - Cl]; UV/vis (CH₂Cl₂) λ_{\max} (log ϵ) 234 (4.53), 349 (4.08), 533 nm (4.23); UV/vis (toluene) λ_{\max} (log ϵ) 280 (4.20), 345 (4.07), 531 nm (4.26); ¹H NMR (CD₂Cl₂, 250 MHz) δ (ppm) 1.84 (s, 3H, Me³), 2.19 (s, 6H, 2 \times Me^{Tol}), 2.20 (s, 3H, Me³), 2.49 (s, 3H, Me⁵), 2.57 (s, 3H, Me⁵), 5.97 (s, 1H, H⁴), 6.03 (s, 1H, H⁴), 6.60 (s, 1H, CH), 6.98 (d, 4H, J_{HH} = 7.9 Hz, *m*-Tol), 7.19 (m, 6H, *m*-PPh₃), 7.33 (m, 3H, *p*-PPh₃), 7.47 (m, 10H, *o*-Tol, *o*-PPh₃); ¹³C NMR (CD₂Cl₂, 62.9 MHz) δ (ppm) 11.3 (Me⁵), 11.5 (Me⁵), 13.7 (Me³), 14.4 (Me³), 22.0 (2 \times Me^{Tol}), 69.2 (CH), 108.5 (br, C⁴), 109.2 (C⁴), 127.9 (d, ³J_{CP} = 9.5, *m*-PPh₃), 129.5 (*o*-Tol), 129.9 (*m*-Tol), 129.9 (*p*-PPh₃), 133.9 (d, ¹J_{CP} = 46.1 Hz, *i*-PPh₃), 134.6 (d, ²J_{CP} = 9.1 Hz, *o*-PPh₃), 139.8 (*p*-Tol), 140.3 (C⁵), 141.6 (C⁵), 142.5 (C _{γ}), 144.0 (*i*-Tol), 155.0 (C³), 155.9 (C³), 166.5 (CO₂⁻), 220.0 (C _{β}), 299.0 (C _{α}), ²J_{CP} = 26.1 Hz); ³¹P NMR (CDCl₃, 161.9 MHz) δ (ppm) 38.1. Red isomer **5b-**

II: mp 213 °C dec; IR (CH₂Cl₂) $\tilde{\nu}$ 1918 w (C=C=C), 1665 s (CO₂⁻), 1650 sh, 1604 w, 1564 w (C=N), 1484 w, 1464 w, 1436 w cm⁻¹; MS FAB (NBOH matrix) *m/z* (relative intensity) 864 (100) [M⁺], 829 (30) [M⁺ - Cl]; UV/vis (CH₂Cl₂) λ_{\max} (log ϵ) 233 (4.52), 347 (4.03), 507 nm (4.24); UV/vis (toluene) λ_{\max} (log ϵ) 280 (4.19), 339 (4.01), 509 nm (4.23); ¹H NMR (CD₂Cl₂, 600 MHz) δ (ppm) 1.35 (s, 3H, Me³), 2.15 (s, 3H, Me³), 2.18 (s, 6H, 2 \times Me^{Tol}), 2.47 (s, 3H, Me⁵), 2.51 (s, 3H, Me⁵), 5.72 (s, 1H, H⁴), 5.86 (s, 1H, H⁴), 6.64 (s, 1H, CH), 7.01 (d, 4H, J_{HH} = 7.9 Hz, *m*-Tol), 7.11 (m, 6H, *m*-PPh₃), 7.23 (m, 3H, *p*-PPh₃), 7.55 (m, 10H, *o*-Tol, *o*-PPh₃); ¹³C NMR (CD₂Cl₂, 150 MHz) δ (ppm) 11.2 (Me⁵), 11.8 (Me⁵), 13.8 (Me³), 14.4 (Me³), 22.0 (2 \times Me^{Tol}), 69.8 (CH), 108.2 (C⁴), 108.5 (C⁴), 127.8 (d, ³J_{CP} = 9.6, *m*-PPh₃), 129.8 (*o*-Tol, *p*-PPh₃), 129.9 (*m*-Tol), 133.6 (d, ¹J_{CP} = 46.2 Hz, *i*-PPh₃), 134.6 (d, ²J_{CP} = 9.3 Hz, *o*-PPh₃), 140.4 (*p*-Tol, C⁵), 142.4 (C⁵), 144.5 (*i*-Tol), 150.0 (C _{γ}), 154.7 (C³), 156.0 (C³), 166.0 (CO₂⁻), 232.8 (C _{β}), 311.0 (d, ²J_{CP} = 18.8 Hz, C _{α}); ³¹P NMR (CDCl₃, 161.9 MHz) δ (ppm) 33.7.

Catalytic Tests (RCM of Diethyl Diallylmalonate). Two-necked flasks (10 mL) equipped with a condenser, argon inlet, and silicone membrane were charged with CH₂Cl₂ (or benzene) (2 mL), decane (internal standard), and diethyl diallylmalonate (10 μ L, 4.13 \times 10⁻⁵ mol). The mixture was heated to reflux, and the ruthenium complex (2.06 \times 10⁻⁶ mol) was added under argon. The reaction was run under reflux for 12 h. The composition of the reaction mixture was controlled by gas chromatography. In separate experiments CuCl (1.30 \times 10⁻⁵ mol) as a phosphine scavenger was added directly after addition of the ruthenium complex.

Calculations. All DFT calculations and full geometry optimizations were carried out by using Jaguar 6.0012⁵⁹ running on Linux 2.4.18-14smp on five Athlon MP 2800+ dual-processor workstations (Beowulf-cluster) parallelized with MPICH 1.2.4. X-ray structures were used as starting geometries. Complete geometry optimizations were carried out on the implemented LACVP* (Hay-Wadt ECP basis on heavy atoms, N31G6* for all other atoms) basis set and the BP86 density functional. Orbital plots⁶⁰ were obtained using Maestro 7.0.113, the graphical interface of Jaguar.

Rotational barriers have been calculated fully relaxed, fixing one torsion angle around the rotated bond and optimizing all remaining degrees of freedom. Torsion angles were modified in steps of 10° beginning from the structure of minimum energy.

X-ray Structure Determinations. Single crystals of **2b**, **3**, **4b-I**, **5a-I**, and **5a-II** were placed at room temperature with Paratone-N onto glass fibers. A modified Siemens P4 diffractometer and an Enraf-Nonius CAD4-Mach3 diffractometer were used for data collection (graphite monochromator, Mo K α radiation, λ = 0.710 73 Å, scan rate 4–30° min⁻¹ in ω). The structures were solved by using either direct methods or Patterson methods (Siemens SHELXS-93⁶¹) and refined with full-matrix least squares against *F*² (Siemens SHELXL-97⁶¹). A weighting scheme was applied in the last steps of the refinement with $w = 1/[\sigma^2(F_o^2) + (aP)^2 + bP]$ and $P = [2F_c^2 + \text{Max}(F_o^2, 0)]/3$. The β -hydrogen atom of **2b** was found and refined isotropically and freely. The other hydrogen atoms were included in their calculated positions and refined in a “riding model”. In the asymmetric units of **2b**, **3**, and **5a-II** the cocrystallized molecules of dichloromethane were included in the models and refined anisotropically. Crystals of **2b** are thin plates. This causes a poor reflection-to-parameter ratio and might explain the high *R* values in the case of **2b**. Nevertheless, an anisotropic refinement of **2b** was possible by applying restraints. One and a half molecules of CHCl₃ crystallized with two molecules of **5a-I** per asymmetric unit. Due to disordered CHCl₃, several restraints had to be applied. The structure diagrams were prepared with the program Diamond

(59) Jaguar, version 6.0; Schrödinger, LLC, New York, 2005.

(60) Stowasser, R.; Hoffmann, R. *J. Am. Chem. Soc.* **1999**, *121*, 3414–3420.

(61) Sheldrick, G. M. SHELX-97, Programs for Crystal Structure Analysis, University of Göttingen, Göttingen, Germany, 1997.

Table 5. Structure Determination Details of Compounds 2d, 3, 4b-I, 5a-I, and 5a-II

	2b	3	4b-I	5a-I	5a-II
empirical formula	C ₃₉ H ₃₈ ClN ₄ O ₂ PRu	C ₃₁ H ₃₀ ClN ₄ O ₃ PRu	C ₃₅ H ₃₈ ClN ₄ O ₃ PRu	2 C ₄₅ H ₄₀ ClN ₄ O ₂ PRu	C ₄₅ H ₄₀ ClN ₄ O ₂ PRu
solvent	CH ₂ Cl ₂	CH ₂ Cl ₂		1.5 CHCl ₃	2 CH ₂ Cl ₂
formula wt	847.15	759.01	730.18	1851.66	1006.15
cryst color, habit	orange, plate	yellow, prism	orange, block	purple, block	red, block
cryst syst	monoclinic	triclinic	monoclinic	triclinic	triclinic
space group, Z	<i>P</i> 2 ₁ / <i>c</i> , 4	<i>P</i> 1̄, 2	<i>P</i> 2 ₁ / <i>n</i> , 4	<i>P</i> 1̄, 2	<i>P</i> 1̄, 2
<i>a</i> (Å)	18.722(11)	10.059(5)	10.254(3)	12.445(11)	12.451(4)
<i>b</i> (Å)	8.699(4)	11.478(4)	14.407(6)	15.072(8)	12.551(7)
<i>c</i> (Å)	24.360(14)	15.463(4)	22.050(8)	25.059(11)	14.899(9)
α (deg)	90	82.190(14)	90	87.26(4)	91.81(4)
β (deg)	99.21(4)	71.12(3)	92.597(18)	77.12(3)	99.29(3)
γ (deg)	90	78.79(2)	90	80.99(4)	101.42(3)
<i>V</i> (Å ³)	3916(4)	1652.0(11)	3254(2)	4525(4)	2247(2)
θ (deg)	2.16–25.00	1.40–24.99	2.15–26.99	2.01–27.00	2.09–26.00
<i>h</i> min, max	–22, 1	–2, 11	–13, 0	–15, 15	–15, 5
<i>k</i> min, max	–1, 10	–13, 13	–18, 0	–19, 19	–15, 15
<i>l</i> min, max	–28, 28	–17, 18	–28, 28	–31, 31	–18, 18
μ(Mo Kα) (mm ^{–1})	0.686	0.805	0.655	0.614	0.725
cryst size (mm)	0.3 × 0.2 × 0.07	0.58 × 0.35 × 0.23	0.2 × 0.2 × 0.2	0.4 × 0.3 × 0.3	0.5 × 0.3 × 0.2
<i>D</i> _c (g cm ^{–3})	1.437	1.526	1.491	1.359	1.487
<i>T</i> (K)	188(2)	158(2)	188(2)	188(2)	188(2)
no. of rflns collected	8637	6203	7497	20 677	9931
no. of indep rflns	6889	5805	7101	19 220	8834
no. of obsd rflns (>2σ(<i>I</i>))	4736	5127	5683	15 202	6322
no. of params	464	397	406	1045	541
no. of restraints	37	0	0	42	0
wt param <i>a</i>	0.0079	0.0602	0.0489	0.1048	0.0409
wt param <i>b</i>	149.8727	6.0853	2.4113	17.6395	4.9484
R1 (obsd)	0.1011	0.0434	0.0429	0.0742	0.0542
R1 (overall)	0.1450	0.0524	0.0608	0.0934	0.0918
wR2 (obsd)	0.2501	0.1251	0.0980	0.1937	0.1088
wR2 (overall)	0.2732	0.1305	0.1064	0.2087	0.1238
diff peak/hole (e/Å ³)	2.921/–0.952	0.983/–1.526	1.198/–0.556	2.732/–1.877	1.681/–1.475

2.1e.⁶² All details and parameters of the measurements are summarized in Table 5.

Acknowledgment. Generous financial support by the Fonds der Chemischen Industrie (Liebig-Stipendium to N.B.) is gratefully acknowledged. Special thanks are due to Prof. Dr. H. Fischer for support and discussion. We are indebted to Mr.

Galetskiy for recording mass spectra and Ms. Friemel for some 2D NMR experiments. We acknowledge a generous gift of ruthenium trichloride hydrate by Degussa AG.

Supporting Information Available: Tables of atomic coordinates and thermal parameters, all bond distances and angles, and experimental data for all structurally characterized complexes as CIF files. This material is available free of charge via the Internet at <http://pubs.acs.org>.

(62) Brandenburg, K.; Berndt, M. Diamond-Visual Crystal Structure Information System; Crystal Impact GbR, Bonn, Germany, 1999. For a software review see: Pennington, W. T. *J. Appl. Crystallogr.* **1999**, *32*, 1028–1029.

OM060050Y